2012

Evaluation of airborne particle emissions from commercial products containing carbon nanotubes

Guannan Huang
University of Iowa

EVALUATION OF AIRBORNE PARTICLE EMISSIONS FROM COMMERCIAL PRODUCTS CONTAINING CARBON NANOTUBES

by

Guannan Huang

A thesis submitted in partial fulfillment
of the requirements for the Master of
Science degree in Occupational and Environmental Health
in the Graduate College of
The University of Iowa

May 2012

Thesis Supervisor: Associate Professor Thomas Peters

Graduate College
The University of Iowa
Iowa City, Iowa

CERTIFICATE OF APPROVAL

_____

MASTER'S THESIS

_____

This is to certify that the Master's thesis of

Guannan Huang

has been approved by the Examining Committee for the thesis requirement for the Master of Science degree in Occupational and Environmental Health at the May 2012 graduation.

Thesis Committee: _____
Thomas M. Peters, Thesis Supervisor

_____
T. Renee Anthony

_____
Patrick O'Shaughnessy

ACKNOWLEDGMENTS

I would firstly like to thank my parents for raising me up and constantly sail behind me in my life. It is hard to overstate my heartfelt appreciation to my academic advisor, Dr. Tom Peters, for guidance and support in everything including professionalism and scientific communication, to name a few, as well as his encouragement, patience and immerse knowledge. My sincere gratitude also goes to my thesis committee members Dr. T. Renee Anthony for the thorough feedback at very tiny detail in my thesis as well as the wise advices in English language usage, and Dr. Patrick O'Shaughnessy for the insightful comments on the overview of my thesis and great suggestions on the statistics, with whose help I developed a better understanding of my research project. I extend my gratitude to the postdoctoral fellows in Dr. Peters' research group, Dr. Cena Lorenzo and Dr. Jae Hong Park for the great assistance on apparatus setup, data collection, microscopy analysis, and thesis proofreading. I would like to thank an anonymous company for providing the test samples. I am indebted to my lifelong friend Ni (Jenny) Zhang for the giving a positive social support on my academia, providing a fun yet stimulating environment in which I learn and grow, as well as caring me in my life, without whom I might have been lost. I would like to express my thanks to all my colleagues and friends in the occupational and environmental health and industrial hygiene program in The University of Iowa for contributing to a friendly and supportive environment.

ABSTRACT

In this study, we developed and standardized a sanding method to evaluate the emission of airborne particles from products that contain carbon nanotubes (CNTs) under different conditions, including three types of sandpaper and three sanding disc speed. We also characterized the emission of the airborne particles from one neat epoxy test sample, four CNTs-incorporating test samples with different CNTs loading, and two commercial products. The total number concentration, respirable mass concentration, and particle size number/mass distribution of the emitted particles were calculated and compared, followed by an electron microscopy (EM) analysis. These data suggest that the sanding process can produce substantial quantities of airborne particles. Also, the emission of airborne particles was associated with different test conditions. EM analysis of the airborne particle samples showed embedded CNTs protruding from the outer surface, which was different from CNTs-incorporating bulk material. Our study suggests a potential generation of particles during the life cycle event of sanding. Further studies should be carried out to investigate the potential human health hazard in other life cycle events.

TABLE OF CONTENTS

LISTS OF TABLES v

LISTS OF FIGURES vi

CHAPTER 1 INTRODUCTION 1

Nanomaterials 1
Health Effects 2
Medical Surveillance 4
Life Cycle Assessment (LCA) 4
Health-Based Exposure Limits 7
Characterization of Airborne Particles Released from Materials during Life Cycle Events 8
Shortcomings of Literature 14
Objectives 14

CHAPTER 2 EXPERIMENTAL STUDY 15

Introduction 15
Methods 17
Results 24
Discussion 29
Conclusion 33

CHAPTER 3 CONCLUSION 45

REFERENCES 47

APPENDIX A TEST PROTOCOL 53

APPENDIX B PRECISION TEST 63

APPENDIX C THE MEAN OF NUMBER CONCENTRATION AND RESPIRABLE MASS CONCENTRATION WITHIN EACH REPETITION UNDER DIFFERENT TEST CONDITIONS 64

LIST OF TABLES

Table 1. Test conditions. 35

Table 2. Comparison of number concentration mean between different test conditions using one-way ANOVA and multiple comparison with Tukey's test at alpha=0.05. P<0.001 36

Table 3. Comparison of respirable mass concentration mean between different test conditions using one-way ANOVA and multiple comparison with Tukey's test at alpha=0.05. P<0.001 37

Table A1.The numbers on the potentiometer related to the actual carriage speed. 60

Table C1. The mean of number concentration and respirable mass concentration within each repetition under different test conditions. 64

LIST OF FIGURES

Figure 1. Experimental setup. 38

Figure 2. Disc sander and lathe. 39

Figure 3. Boxplots of (a) number concentration and (b) respirable mass concentration and particle size distribution of (c) number and (d) mass for percentages of CNTs when using the medium disc sander and the medium sandpaper grit. 40

Figure 4. Boxplots of (a) number concentration and (b) respirable mass concentration and particle size distribution of (c) number and (d) mass for sanding disc speed when using the 2% CNTs test sample and the medium sandpaper grit. 41

Figure 5. Boxplots of (a) number concentration and (b) respirable mass concentration and particle size distribution of (c) number and (d) mass for roughness of sandpaper when using the 2% CNTs test sample and the medium disc sander speed. 42

Figure 6. Boxplots of (a) number concentration and (b) respirable mass concentration and particle size distribution of (c) number and (d) mass for different test samples when using the medium disc sander speed and the medium sandpaper grit. 43

Figure 7. Microscopy images including (a) SEM image and (b) TEM image of 2% CNTs-epoxy nanocomposite particle. 44

Figure A1. The setup of the whole system. 54

Figure A2. The motor pulley and the drive pulley 55

Figure A3. Rate set at 9.0 55

Figure A4. Test sample mounted on the carriage. 56

Figure A5. The air movers switched on. 56

Figure A6. The pressure inside the cabinet. 56

Figure A7. The linear regression between the number on the potentiometer and actual carriage speed. 61

CHAPTER 1

INTRODUCTION

Nanomaterials

Nanomaterials are objects with one, two, or three dimensions in the size range of 1-100 nm (ISO, 2007). They have been at the forefront of science and technology since fullerene (C_{60} molecule) was discovered in 1985 (Kroto et al., 1985). In later studies, carbon nanotubes (CNTs), including single-wall carbon nanotubes (SWCNTs) and multi-wall carbon nanotubes (MWCNTs), were also discovered (Iijima, 1991).

Nanoparticles (NPs) are objects with all three dimensions smaller than 100 nm. They can be divided into two types: incidental NPs or ultrafine particles, those not produced intentionally (such as particles from combustion); and engineered NPs, those intentionally produced (such as TiO_2 NPs). The properties of engineered NPs can be altered by changing their size, shape, or surface coating. These properties may be quite different from the bulk materials and vary when the particle size changes. Some nanomaterials can conduct electricity better than copper, while others have strong tensile strength but are light in weight (Smalley, 1999). Due to the unique size of NPs, nanomaterials have a large surface area relative to their mass so that they can interact with other materials. Thus, nanomaterials incorporating NPs are applied extensively in industries.

CNTs are tiny hollow cylinders ranging in diameter from 0.4 nm to 2.5 nm (Iijima, 1991). They have become the major mass-produced nanomaterials (Donaldson et al., 2006) as a result of their versatility. Due to their unique properties including small dimension, high tensile strength and energy storage capacity, CNTs have been widely

used to reinforce the matrix in the production of tennis rackets and airplane frame parts (Ajayan & Zhou, 2001). In addition, the application of CNTs in polymer composites such as epoxy can enhance the toughness of the composites by absorbing energy during the highly flexible behavior of the polymers. Due to this property, CNTs are applied in ceramic matrix composites (Ajayan & Zhou, 2001).

Health Effects

Extensive studies have been conducted to investigate the toxicology of nanomaterials. Using the search engine PubMed in early 2012 with the search strings nano and toxicity-related terms (i.e., toxicology and toxicity) generated more than 1000 hits with carbon nanotubes and metal-containing NPs the most studied substance. Studies found that the toxicology profile of a nanomaterial originated from the higher surface area and thus increased surface reactivity compared to traditional materials (Hubbs et al., 2011), although material-specific toxicity was often found in some nanomaterials. Inhalation is an essential route of exposure for nanomaterial uptake, which will be talked later. Deposition of inhaled particles depends largely on size; for example, particles with diameter less than 0.01 μm have enhanced deposition in the tracheobronchial region due to the rapid Brownian motion of the particles (Hinds, 1998). Dermal exposures to nanomaterials have been found to be an issue in workers (Hubbs et al., 2011), but there is no evidence that NPs larger than 20-100 nm could penetrate the skin into living tissues (Warheit et al., 2007). Thus, dermal uptake of NPs in any case is orders of magnitude smaller than inhalation (Warheit et al., 2007), whereas hand-to-mouth contact can pose hazard to workers.

This chapter focuses on the pulmonary and cardiovascular toxicity of inhaled CNTs in both *in vitro* and *in vivo* studies, especially those related to workplace exposure. SWCNTs have been shown to cause acute inflammation, granuloma, and lung fibrosis in exposed rodents (Shvedova et al., 2008, 2005b, 2007), while the same effects were observed for MWCNTs (Muller et al., 2008, 2005; Ma-Hock et al., 2009). In a recent study, human airway epithelial cells were exposed to SWCNTs for 20 weeks at the OSHA Permissible Exposure Limits (PEL) of 5 mg/m^3 (OSHA, 2006) and mitotic spindle aberrations were found, which may suggest that existing workplace limit was not protective for workers (Sargent et al., 2011). Also, for every dose of SWCNTs at 7 $\mu g/m^3$, the risk factor for early-stage pulmonary fibrosis increased by 10 percent (Kuempel, 2011). In addition, a comparative study indicated that SWCNTs were much more potent than crocidolite asbestos and ultrafine carbon black, and SWCNTs were able to give rise to an increased incidence and severity of inflammatory and fibrotic responses in mice (Teeguarden, 2011). In terms of the determinants of CNTs toxicity, a study assessed the impact of coating on CNTs pulmonary toxicity and concluded that MWCNTs cytotoxicity, inflammation, and oxidative stress were enhanced by acid-based coating and decreased by polystyrene-based polymer coating both *in vitro* and *in vivo* (Tabet et al., 2011). Evidence has shown that nanomaterials can impair cardiovascular system in rodents as a result of different mechanisms. Li et al. (2007) investigated the cardiovascular effects of SWCNTs in *in vivo* tests and found an acceleration of plaque formation, an early sign of arthrosclerosis in ApoE(-/-) transgenic mice.

Medical Surveillance

No epidemiological studies were found on how adverse health effects relate to engineered NP exposure, although ultrafine particles are known to induce adverse health outcomes. Epidemiological studies on ultrafine particles can render evidence of personal protection and personal sampling in the NPs context (Peters et al., 2011). In France, a proposed double surveillance system consisted of a prospective cohort survey and repeated cross-sectional studies (Boutou-Kempf et al., 2011). Also, BASF, a global chemical company, successfully identified nanomaterials in use and established a registry of workers handling nanomaterials in the company (David et al., 2011). In addition, Schubauer-Berigan et al. (2011) concluded that half of the 61 companies recruited in their study provided information about material dimensions, quantities, synthesis methods, and worker exposure reduction strategies, which was an essential step toward a successful medical surveillance plan. In addition, larger-scale companies reported greater use of nanomaterial-specific strategies, especially for respiratory protection (Dahm et al., 2011).

Life Cycle Assessment (LCA)

LCA is a concept first proposed by the US Environmental Protection Agency (EPA) (Hunt & Frankli, 1996). It covers the cradle-to-grave analysis of potential impacts that may occur as products undergo various life-cycle events, including manufacturing, transport, use, disposal, and recycling. The National Nanotechnology Initiative (NNI) (2011) has identified the second goal of nanomaterial measurement infrastructure as "developing measurement tools for the detection and monitoring of engineered nanomaterials (ENMs) in realistic exposure media and conditions during the life cycles of ENMs".

An important tool of LCA is life cycle risk assessment (LCRA). There are two essential dimensions of risk — the probability of an event occurring and the magnitude of the consequences (Shatkin, 2008). In the context of nano LCRA, the magnitude of adverse consequences is reflected in the toxicity characterizing the severity, while the probability could be considered as exposure. The absence of exposure could never put one under risk regardless of the toxicity. The exposure to nanomaterials could be determined by the ability of the life cycle process to release airborne particles (discussed below in the characterization of released particles), the process in which nanomaterial is handled (also discussed below), and the application of ventilation and personal protective equipment.

The synthesis of CNTs-containing epoxy may represent an exposure hazard both in pre-mixing processes and polymer compounding (FERA, 2009). CNTs are produced before they are incorporated into polymers. There are three processes of manufacturing: arc discharge or pulsed laser vaporization (Ando et al., 2004), chemical-vapor deposition (CVD) process (Leonhardt, 2004), and laser-oven route (no longer in use). Tsai et al. (2009) studied the field measurements of particles released during CNTs production in a CVD, and observed high concentration of NPs during the SWCNTs and MWCNTs production, while airborne NPs were not detectable at the laboratory background location under a fume hood. In addition to CNTs manufacturing, processes including transfer of pre-cursor materials, batch mixing, extrusion, removal of CNTs-containing polymeric material, and cutting /shaping could induce exposure to CNTs-containing materials (FERA, 2009).

The LCA of CNTs-containing epoxy resin emphasizes processes including use, disposal, and recycling (FERA, 2009). Normal use and handling of CNTs-containing epoxy that do not involve the breakage of nano-product structure are unlikely to cause the release of particles, but the mechanical disruption of CNTs structure (e.g., machining and grinding) can probably cause particle generation, especially when UV light is present (Hsu & Chein, 2007). In regards to disposal, the break-down of CNTs starts at the temperature of 740ºC under oxidative conditions (Köhler et al., 2008). Thus, the disposal of CNTs-containing epoxy under normal conditions is unlikely to pose a hazard to human. Recycling of CNTs-containing nanocomposites and resins, including separating, chemically cleaning, and grinding can give rise to particle release (FERA, 2009).

The LCA of other CNTs-containing materials share some similarities with CNTs-containing epoxy resins. Köhler et al. (2008) studied CNTs release during different processes for CNTs-containing Li-ion batteries and textiles. Exposure to particles through the use of Li-ion batteries may be attributed to operation by the user (by applying mechanical force or exposure to heat) and irregular recharge attempts. The use of CNTs-containing textiles could induce the degradation of polymers by external chemical and from physical influences such as extreme temperature and UV light. Uncontrolled disposal by fire is most likely to release CNTs. Sophisticated methods of recycling including milling, grinding and thermal treatment could cause CNTs release as well (Köhler et al., 2008).

Previous studies identified that CNTs posed a risk only after being aerosolized (FERA, 2009). Thus, the study of sanding CNTs-containing products is essential in LCA since this process appears in both use and recycling process. In that sense, it is imperative

to look at the particle release in sanding process, especially under different conditions (e.g., sanding speed, sandpaper use, and the presence of UV light).

Health-Based Exposure Limits

The National Institute for Occupational Safety and Health (NIOSH) has set the recommended exposure limit (REL) of 7 $\mu g/m^3$ elemental carbon as an 8-hour TWA respirable mass airborne concentration based on the upper limit of quantification of NIOSH method 5040. Although REL is at the lowest airborne CNTs concentration that can be accurately measured, it is likely that concentration below this level would cause adverse effect (NIOSH, 2010).

Many nanomaterials, including CNTs and alumina NPs, are considered as "chemical substances" under the EPA Toxic Substances Control Act (TSCA). Since 2008, EPA requires manufacturers of new chemical substances to provide specific information for review prior to manufacturing chemicals or introducing them into commerce. Also, EPA is developing a Significant New Use Rule, which requires persons intending to manufacture, import, or process new nanomaterials listed on the TSCA inventory to submit a Significant New Use Notice to EPA at least 90 days before commencing that activity (EPA, 2011). This act would prompt a comprehensive risk assessment profile of nanomaterials used during processing to protect workers. However, no specific exposure limits have been implemented due to a lack of quantitative data.

Hazardous exposures associated with nanomaterial are generally regulated under the OSHA Occupational Safety and Health Standards, which regulates nanomaterial exposure according to their chemical composition (e.g., iron oxide fume PEL=10 mg/L, titanium dioxide PEL=15 mg/L). Meanwhile, inert NPs composed of carbon are covered

under Particulates Not Otherwise Regulated (PNOR) category with PEL of 15 mg/m^3 for respirable fraction and 5 mg/m^3 for total dust as an 8-hour TWA (OSHA, 2011).

American Conference of Governmental Industrial Hygienists (ACGIH) do not have nanomaterial-specific limit, either. Airborne nanomaterials are regulated under Chemical Specified Particle Threshold Limit Values (TLVs), which are developed from hazard assessments based on larger particle exposures, or respirable TLV for particle not otherwise specified (PNOS TLV-3000 µg/m^3) (ACGIH®, 2011).

Characterization of Airborne Particles Released from Materials during Life Cycle Events

Some studies characterized the particles released from nanomaterials during sanding, while several studies investigated particle release induced by sanding in materials beside nanomaterials. Others simulated life-cycle events under conditions such as light and mechanical wearing to assess the particle generation. It was desirable to separate the nano-incorporated matrix from the surface coating matrix, since the likelihood and form of release was determined by how CNTs were incorporated into the material (Köhler et al., 2008). Measurements usually included particle number/mass concentration, particle size distribution, and mass loss of the nanocomposite. Electron microscopy (EM) and spectroscopy analysis often revealed the physical characteristics of released particles. Since the sampling was often taken in the neighborhood of particle production, it represented the worst-case scenario of particle generation (Göhler et al., 2010). Therefore, these studies might be useful to assess possible particle emission of nanomaterial products in the workplace.

Release from Nanomaterials in Matrices and Surface Coatings

From sanding

A broad range of studies have investigated particle emission during the sanding process. Bello et al. (2008) investigated the abrasive machining of CNTs-composites and found a significant release of NPs during dry cutting, whereas wet cutting did not produce concentration significantly higher than background. Hsu & Chein (2007) compared the impact of different activities by monitoring the release of TiO_2 NPs coated on a variety of substrates. They found that a scraping motion could induce the generation of NPs as UV light deteriorated the organic compounds in the coating agent. The release of particles in different substrates under various conditions was confirmed by other studies (Wohlleben et al, 2011). Further, Göhler et al. (2010) found particle number concentration density changed over time and attributed the change to uncertainties (e.g., reproducibility of test condition and/or the formation of agglomerates). However, Cena & Peters (2011) did not find a significant increase in the total number concentration during sanding CNTs-incorporated epoxy compared to the background concentration, while there was a six-fold increase of the respirable sized particle number.

Other researchers have compared airborne particles released when materials with NPs and without NPs are sanded. Koponen et al. (2009) found that the addition of NPs only caused a minor difference of the geometric mean diameter of particles released from the sanding of NP-containing paints, and the emission varied with the type of the paint. In addition, Bello et al. (2008) found no significant impact of CNTs-composites on the particle generation tendency during dry cutting. Studying particle release from surface

coatings, Göhler et al. (2010) further confirmed that particle number concentration did not depend on the presence of nano-additives but on the employed coating material. Wohlleben et al. (2011) also found no substantial increase in particle number and mass concentration due to the addition of nanofiller to the material, while the rigidity of material may play a more important role in determining the particle mass and size distribution. These results were supported by the test with taber abraser that nanocomposites under normal use and wear did not differ significantly from their traditional counterparts without nanocomposites (Wohlleben et al., 2011). In contrast, Raynor et al. (2012) found that shredding of plain resin produced significantly higher amount of particle number than shredding of nanoclay-filled plaques.

Among a few studies examining particle size distribution and its determinants, Koponen et al. (2009) found that particles smaller than 50 nm dominated the number concentration distribution, whereas the small particles only played a minor role on mass and surface area distribution. These particles originated from the sander rather than the material. Also, the size of the observed number concentration modes was most likely to depend on factors such as sandpaper grit size and the sander speed (Koponen et al., 2009). Cena & Peters (2011) concluded that particles from manual sanding were predominantly larger than 300 nm while no nano-sized particles were found. Bello et al. (2008) found the number concentration of particles from machining had a polydisperse distribution, and the peak varied by composite type. Göhler et al. (2010) concluded that the particle size distribution was constant over time during sanding surface coating.

Some studies examined the mass loss of the material being sanded during the sanding process. Vorbau et al. (2009) investigated the sanding of surface coating and

concluded that the mass loss depends on the carrier material and coating. Plus, it was impossible to correlate the mass loss with the particle number due to the different mechanical rigidity of carrier materials. This was further supported by Göhler et al. (2010).

While the sander and sandpaper could produce particles from nanomaterial through mechanical breakage, they may also account for more properties in particle release. Koponen et al. (2009) found that the sander was the only source of particles smaller than 50 nm. Wohlleben et al. (2011) identified that the dispersing of abraded material was not a continuous process, as the abraded particles may collect on the sandpaper and be released periodically in larger quantities. In addition, when sanding hard specimens, particles from the sandpaper accounted for the respirable fraction of particles generated. Göhler et al. (2010), in contradiction, found no abrasive particles removed from abrasive paper's surface.

Questions were raised in regards to the presence of CNTs in particle production as well as their form of release. Cena & Peters (2011) found no CNTs free from CNTs-incorporated epoxy composite in manual sanding studies, which was confirmed by Vorbau et al. (2009) and Göhler et al. (2010). Cena & Peters (2011) further concluded that the morphology of particles generated during the sanding of CNTs-epoxy nanocomposites was very different from the bulk CNTs. Bello et al. (2008), however did not observe CNTs in extensive EM studies of the particle samples.

From processes other than sanding

Some studies looked at handling processes other than sanding in terms of particle release. Wohlleben et al. (2011) investigated the effect of weathering (UV light) on

nanomaterial and observed no significant release of particles. They also found chalking was an issue for organic nanocomposites. Hsu & Chein (2007) simulated various life cycle events on surface coating and concluded that compared to a fluorescent lamp, UV light had a more serious effect on the coating. Cena & Peters (2011) looked at particle release during weighing and found that the respirable sized particle number was 1.79 times higher than background, while there was no significant increase in the total number concentration. Tsai et al. (2009) investigated the nanosilver and nanoalumina particle release of pouring and transferring from beaker to beaker by spatula under the fume hood, and observed a significant increase of airborne NPs in the laboratory and in the researchers' breathing zone. Tsai et al. (2009) concluded that pouring generated more airborne particles than transferring, but the particle number concentration in the breathing zone was not affected simply by handling method. Further studies should be carried out to investigate particle release in various scenarios under different conditions before the large-scale handling of nanomaterials are carried out.

Processes with Materials Other Than CNTs

Wood dust

Since literature that looked at the emission from nanomaterials is limited, it would be helpful to extrapolate from preexisting data from material other than CNTs. Wood dust is known to produce high dust emission (Thorpe & Brown, 1994) and cause lung cancer in sawmill workers (Bhatty et al., 2011). In previous studies, personal exposures to wood dust during different wood-working activities were higher than the proposed health-based limit of 0.2 mg m^{-3} in Netherland (Scheeper et al., 1994), whereas a recent study has shown that the total dust mass concentration was lower than OSHA PEL

(Welling et al., 2009) during wood sanding. However, another study that looked at wood dust release in both outdoor and indoor construction sites observed exposures to metals like arsenic, which are used as wood preservatives (Decker et al., 2002). A variation of airborne particle concentration was also found; the airborne particle concentration only accounted for a small fraction of total particle mass concentration in some studies (Decker et al., 2002), while it accounted for a greater fraction in particle number concentration in other studies (Welling et al., 2008). In studies that looked at the association of sandpaper and particle number and mass concentration, sanding with coarse sandpaper produced significantly higher amount of particles than sandpaper with fine grits (Welling et al., 2008). In terms of workplace exposure elimination, control strategies including sanding with the presence of ventilation, vacuum cleaning of machines, and cleaning staff led to a 7% annual decline in dust mass concentration (Schlunssen et al., 2008).

Asbestos fiber

Operations with asbestos have long been known to create high levels of airborne asbestos dust (Verma & Middleton, 1980), which may render evidence to CNTs exposure. Recent studies, however, showed the opposite. Mowat et al. (2005) investigated the release of asbestos fibers from processes including band sawing, belt sanding, and press drilling. They found 8-hour TWA exposure was fifty-fold less than OSHA PEL of 2 f/cc. Similar results were obtained in another study investigating asbestos-containing fibered roof substrates and plastic cements during hand sanding and hand scraping activities (Mowat et al., 2007). Paustenbach et al. (2004), in addition,

estimated 8-hour TWA to be no greater than 0.009 fibers/cc during the application, sanding, and cleanup of four different asbestos-containing products.

Shortcomings of Literature

There are not a lot of studies that examined the exposure to CNTs from sanding on CNTs-containing epoxy resin. Other limitations of previous sanding studies with CNTs may include uncertainties inherent in the test leading to a lack of reproducibility. A lack of comparability might also be an issue in literature since only a few studies applied standardized methodologies.

Objectives

This work will establish the feasibility of conducting tests on products that contain engineered nanomaterials. The objectives of this thesis are: (1) to develop a method to characterize the emission of airborne particle release from CNTs-incorporated epoxy test samples and commercial products when they undergo life cycle events of sanding; and (2) to compare the emitted particle number/mass concentration, particle size distribution, and airborne particle morphology under different test conditions such as varying the sanding disc speed, the sandpaper grit, and the test samples used. Further, the aim of this work is to establish a standard method that can 1) be modified for any nanocomposite product, 2) serve as a model for extension to other life cycle events and degradation factors, and 3) function as a front end for toxicity testing of environmentally-relevant aerosols.

CHAPTER 2

EXPERIMENTAL STUDY

Introduction

Nanomaterials, materials incorporating objects with one, two, or three dimensions in the size range of 1-100 nm (ISO, 2007), have been extensively studied because of their unusual physicochemical, mechanical, and electrical properties as well as their broad range of potential applications. The increase in commercial interest and subsequent mass production will lead to greater possibilities for interactions of CNTs with humans and the environment. A life cycle risk assessment is an important tool of nano LCA and involves assessing the magnitude (i.e., the toxicity) and the possibility (i.e., the exposure) of nanomaterials (Shatkin, 2008).

The toxicology profile of CNTs is not fully understood yet. The pulmonary toxicity is a major adverse effect in workplaces. Inhalation exposure is an essential route for nanomaterial uptake; in this process, the particle size is the major determinant for deposition in the respiratory tract (Hinds, 1998). Acute inflammation, granuloma, and lung fibrosis were found in rodents exposed to either SWCNTs or MWCNTs in animal tests (Shvedova et al., 2008, 2005b, 2007; Muller et al., 2008, 2005; Ma-Hock et al., 2009). In addition, human epithelial cells were exposed to CNTs at concentrations equal to the OSHA PEL, and mitotic spindle aberrations were found (Sargent et al., 2011), suggesting existing standard not protective for workers.

Manufacturing processes, including pre-mixing and polymer compounding, could be a source of nanomaterial exposure, while the use of CNTs products involving mechanical disruption of CNTs structure and recycling processes including separating,

chemically cleaning, and grinding can give rise to particle release (FERA, 2009). In terms of human exposure to nanomaterials in workplace, the particles emission from nanomaterials during the sanding process was characterized in recent studies. Since the area sampling was taken in the neighborhood of particle production, it represented the worst-case scenario of particle generation (Göhler et al., 2010). In nanocomposite sanding tests, the generation of NPs was found (Bello et al., 2008; Hsu & Chein, 2007), and the particle emission from different substrates under various conditions was reported by Wohlleben et al. (2011). However, a significant increase in the total number concentration during sanding process compared to background was not shown in study by Cena and Peters (2011). Regarding to the addition of nanocomposites, Bello et al. (2008) and Wohlleben et al. (2011) found no significant change in airborne concentrations during dry cutting CNTs-composites; however, Wohlleben et al. (2011) concluded that rigidity of material played an important role in determining the particle mass and size distribution. Koponen et al. (2009) studied the size distribution as well as its determinants; they found that particles smaller than 50 nm dominated the number concentration distribution, whereas the nano-sized particles only played a minor role on mass and surface area distribution. However, these particles originated from the sander rather than the material being sanded. Also the size of the observed number concentration modes was most likely to depend on factors such as sandpaper grit size and the sander speed (Koponen et al., 2009).

There are not a lot of studies that examined the exposure to CNTs from sanding on CNTs-containing epoxy resin, and the reproducibility was low in previous studies. A lack of comparability between different studies might also be an issue since only a few

studies applied standardized methodologies. Thus, the objectives of this study is: (1) to develop the method that was designed to characterize the emission of airborne particles from CNTs-incorporated epoxy test samples, as well as commercial products, through a sanding process; and (2) to compare the particle number/mass concentration, particle size distribution, and airborne particle morphology under different test conditions such as varying the sanding speed, the sandpaper grit, and the test samples used.

Methods

Experimental Apparatus

As shown in Figure 1, the experimental setup consisted of a sand blasting cabinet and a sampling/measurement system. The cabinet (Item 93608, Central Pneumatic, Byron Center, MI, US) was fixed inside a plastic enclosure (1 m × 0.7 m × 1 m) which prevented the particles in the room air from leaking into the cabinet. A commercial lathe (L1015, Taig Tools, Chandler, AZ, US) was installed inside the cabinet to simulate sanding. The clean air from a high-efficiency particulate air (HEPA) filtered air blower (#1 in Figure 1; CM3000, Fantech, Lexena, KS, US) was supplied to the plastic enclosure by a variable voltage regulator (TDGC-2kVA, Johsun Tec, Zhejiang, China) at the flow rate of 0.14 m^3/s (300 ft^3/min). The clean air from an identical HEPA filtered air blower (#2 in Figure 1) was supplied to the cabinet by an identical variable voltage regulator at the flow rate of 0.12 m^3/s (250 ft^3/min) to maintain a negative pressure. A valve-controlled local exhaust system was used to extract the air from the cabinet. A second exhaust pump (Air Sampling Pump, 6P-280, Air Diagnostics and Engineering Inc., Naples, ME, US) was used to extract the exhaust air at 22.45 L/min that passed through a sampling manifold to which measurements and samples were attached to.

The airborne particles from the cabinet were monitored and sampled from the manifold. An airborne particle sample was collected on a 0.4-μm-pore polycarbonate filter (E0413-MB, Structure Probe, Inc., West Chester, PA, US) using a sampling pump (Universal Sample Pump, 224-PCXR4, SKC Inc., Eighty Four, PA, US) at the sampling flow rate of 1 L/min within each sanding test run. The morphology of the collected airborne particles was characterized by a scanning electron microscopy (SEM; S-4800; Hitachi High Technologies, Inc., Schaumburg, IL, US) and a transmission electron microscopy (TEM; JEM-1230; JEOL USA Inc., Peabody, Mass., US). During the SEM sample preparation, the sampling filter was placed on a carbon tape which was attached to an aluminum stub, coated with a sputter coater (K550, Emitech, Ashford, UK), and analyzed under SEM. For TEM sample, the airborne particles were dispersed in acetone and then dipped on a TEM grid. The grid was air-dried and analyzed with TEM. The results of the microscopic analysis are presented in the result part.

The particle concentration in the sampling manifold was monitored with direct reading instruments (DRIs) including a condensation particle counter (CPC; 3007, TSI, Shoreview, MN, US) with 1 second time resolution to measure the total number concentration of particles sized between 10 nm and 1 μm in aerodynamic diameter, and an optical particle counter (OPC; PDM-1108, Grimm, Ainring, Germany) with 1 second time resolution to measure the particle number concentration in 15 channels from 0.3 μm to 20 μm in optical diameter. The sampling flow rates of the CPC and the OPC were 0.7 L/min and 1.2 L/min, respectively. The number concentrations measured by the CPC and the OPC were used to calculate the respirable mass concentration using the following equation (Peters et al., 2006):

$$M_R = \frac{\pi}{6} d^3_{CPC} \rho N S_R(d_{CPC}) + \sum_{i=1}^{15} \pi \rho d^3_{mid,i} N_{OPC,i} S_R(d_{mid,i})$$

(Eq. 1)

where d_{CPC} is the assumed midpoint diameter of the CPC data, ρ is the particle density (assumed to be 1000 kg/m^3), S_R is a function for the fraction of respirable mass, $d_{mid,i}$ is the midpoint diameter of the OPC channel, i. The midpoint diameter of the CPC data was estimated from scanning mobility particle sizer (SMPS; 5.400, Grimm, Ainring, Germany) measurements. The flow rate for the ultrafine particle counter on the SMPS is 0.3 L/min. The size distribution of the particles was derived by merging data from the SMPS (9.8 nm-847.8 nm) and the OPC (350 nm-25000 nm).

The Simulation of a Sanding Life Cycle Event

The lathe (Figure 2) in the cabinet was used to simulate a sanding life-cycle event. A 10.4-cm diameter disc was attached to the spindle of the lathe. Adhesive-backed sandpapers made of aluminum oxide as abrasive material were affixed to the surface of the disc. The sandpapers have three levels of roughness (ADALOX A290 P80, P150, and P320, Norton Abrasive, Worcester, Mass., US). The disc was driven by an electric motor (Marathon Electric Motor, JVD48S17D2042NK, Marathon Electric, Wausau, WI, US), which was positioned outside the cabinet to avoid particle contamination in the cabinet. The disc speed was controlled by adjusting a pulley outside the cabinet.

Impelled by a turning screw beneath the lathe, the carriage drove the test sample toward the spinning sander at a right angle to the surface of the disc. The carriage was designed to operate in forward (i.e., toward the sander) and backward (i.e., away from the sander) direction, while the carriage speed was adjustable in the range of 0.0017-0.2781 cm/s and was controlled by a potentiometer outside the cabinet. A nanocomposite test

sample was mounted on the tool post on the carriage of the lathe, which fed the sample to the disc sander during test runs.

In this arrangement, the abrasion energy could be modified by varying the sandpaper type, the disc speed, the distance between where the test sample contacts the disc and the center of disc rotation, and the carriage speed. In this project, only the test sample, the sandpaper type, and the disc speed were varied. New sandpaper was installed in every test run, since the consuming of the sandpaper grit may reduce the abrasion energy and thus cause an undesired pause of the disc sander. The carriage speed was kept low and unchanged to prevent the disc sander from dysfunction, which may occur when the feed energy from the carriage is greater than the abrasion energy.

Test Protocol

We defined and standardized a method for characterizing the particles emitted during the mechanical abrasion of CNTs-containing epoxy nanocomposites and commercial products. The complete version of the test protocol can be found in Appendix A. The first four sections of this part were done in every test while the last two sections were achieved only once.

Test condition setup

Before each test run, the disc speed was set by shifting the position of the pulley and was measured by a tachometer (Laser Photo Tachometer, 461920, Extech Instruments Corporation, Waltham, PA, US). The sandpaper on the surface of the disc was peeled off and a new piece of sandpaper was affixed to the disc. With gloves, a test sample was then mounted on the carriage and positioned perpendicular to the face of disc sander at 0.85 inches (2.16 cm) from the outer edge. The carriage speed was set forward

at 0.0025 cm/s with a potentiometer. A filter cassette was then attached to the sampling manifold. Both the HEPA filtered air blowers were set at the required air velocity and switched on to achieve a pressure drop of 30 Pa measured by a magnehelic pressure gauge on the pipe connecting the cabinet and the HEPA filter. A slightly negative static pressure (-25 Pa) was maintained in the cabinet as measured with a pressure gauge by adjusting the cabinet exhaust valve, and a positive pressure was sustained in the plastic enclosure. The DRIs were switched on.

Background concentration measurements

The background concentration measurements started when particle number concentration dropped below 100 particles/cm^3 and respirable mass concentration dropped below 0.05 mg/m^3. Background measurements were taken with the DRIs for 5 minutes prior to any sanding tests.

Process concentration measurements

The sanding process started when the sanding disc and the feed carriage were activated simultaneously and operated at the target rate. This process took about 12 minutes. The first 5.5 minutes were used to stabilize the number and respirable mass concentrations. During the last 6.5 minutes the sampling pump was turned on to take an airborne particle sample on the filter. The particle size distribution was measured by the SMPS over the same period as the airborne particle sample collection. As soon as an SMPS run was completed, the disc sander, the carriage as well as the sampling pump were switched off, and the test run ended.

After test runs

The filter cassette was disconnected to the airflow, and the filter was replaced with a new one. A bulk dust sample was collected by a scoop into a petri dish at the bottom of the cabinet. The remaining dusts in the cabinet were removed by applying a vacuum to the cabinet.

The precision test

The precision test examined the consistency of the test runs regarding to number/respirable mass concentration and particle size distribution. The description and the result of the precision test can be found in Appendix B.

Particle emission when the disc sander is on but the feed is off

In order to clarify the source of airborne particles, tests were performed to investigate the particle emissions when the sander was spinning at the speed of 1425 revolutions per minute (RPM) with P80 sandpaper on it but the test sample was not fed to the disc.

Comparison of particle emissions from CNTs-reinforced epoxy samples

The 11 tests of 1 neat epoxy test sample, 4 CNTs-reinforced epoxy test samples and two commercially available CNTs products are provided in Table 1. The epoxy test samples (Applied Nanotech Inc., Austin, TX, US) were sticks (12.5 cm × 1.3 cm × 0.5 cm) consisting of epoxy and MWCNTs with five percentages (0% - neat epoxy, 1, 2, 3 and 4% by weight of CNTs in epoxy). The test samples composed of neat epoxy were light yellow, whereas those with CNTs added were grey. Basically how these samples were prepared by the manufacturer is by mixing CNTs of 10-50 nm in outer diameter and

1-20 μm in length (Baytubes, Bayer Material Science, LLC, Pittsburg, PA) with epoxy resin, pouring the mixture into a mold and baking it in an oven. Additionally, two commercially available products (manufacturer anonymous) containing CNTs were called Sample 1 and Sample 2, and cut into the similar size as the CNTs-reinforced epoxy test samples. Three sandpaper grit levels (fine, P320, grit sized 46.1 μm in average; medium, P150, grit sized 100 μm in average; and coarse, P80, grit sized 201 μm in average) and three disc speeds (slow, 586 RPM; medium, 1425 RPM; and fast, 2167 RPM) were used. The medium sandpaper grit, the medium disc speed, and 2% CNTs were defined as the standard test conditions. When varying the sandpaper grit, the medium disc speed and 2% CNTs were used; when varying the disc speed, the medium sandpaper grit and 2% CNTs were used; when varying the test samples, the medium sandpaper grit and the medium disc speed were used. All the measurements were performed in triplicate.

For each test sample, the mean of 40 number concentration data points and the mean of 40 respirable mass concentration data points within each triplicate were computed. The three repetitions within one test condition were treated as three observations. Difference of both number concentration and respirable mass concentration mean under one test condition were compared with other test conditions using Analysis of Variance (ANOVA) with Minitab 16 Statistical Software (Minitab Inc., State College, PA, US). A total of four ANOVA analyses were performed: analysis of five test samples with different CNTs percentage, analysis of three 2% CNTs samples with different sandpaper grit, analysis of three 2% CNTs samples under different sander speeds, and analysis of three different types of test samples. The rationale for choosing parametric

tests although the data didn't pass normality tests was that parametric tests provide more statistical power than non-parametric tests. Multiple comparison using Tukey's test at alpha=0.05 was also performed to compare the difference in number and respirable mass concentration mean among all test conditions.

Results

The results under each test condition are summarized in Figure 3 through Figure 6 by boxplots and particle size distributions. For the boxplots, the upper and lower boundary of the boxes indicates the 75^{th} and 25^{th} percentiles, the central line indicates the median, and the whiskers above and below indicate the maximum and minimum of the values. The arithmetic mean of the number concentration from CPC and the computed respirable mass concentration from CPC and OPC of the triplicates as well as the statistical results are presented in Table 2 and Table 3, respectively. The number concentration and respirable mass concentration within each triplicate are provided in Table A2 in Appendix C.

Comparison of particle emissions for CNTs

percentage

Tests conducted with test samples having different CNTs loading are presented in Figure 3. From Panel (a) and (b) of Figure 3, the number concentration was less than 650 particles/cm^3 and the respirable mass concentration was less than 0.4 mg/m^3. Generally there was a rise in number concentration corresponding to the increase of CNTs loading, except for 0% CNTs, which emitted higher amount of particles than 1%, 2%, and 3% CNTs in average. The breakage of 4% CNTs produced the most particles, with the mean of 455 particles/cm^3 and the maximum of 634 particles/cm^3. From Table 2 and Table 3,

the difference in number concentration for 4% CNTs was statistically different from that of 1% CNTs, 2% CNTs, and 3% CNTs. The respirable mass concentration increased with the CNTs percentage as well, although 3% CNTs produced smaller amount of respirable mass compared to 0%, 1%, and 2% CNTs. Again, 4% CNTs emitted the greatest amount of respirable mass concentration, which was significantly different from those from other CNTs percentages, and its mean was almost three times of the mean for 3% CNTs.

The five test samples produced similar particle size distributions as illustrated by Panel (c) and (d) of Figure 3; they had two modes and peaked at the similar particle diameter, one smaller than 100 nm and the other between 500 nm and 5 μm. The number size distribution was dominated by particles sized smaller than 100 nm. In the size range larger than 1 μm, the particle number concentrations were less than 20 particles/cm^3 except for the 4% CNTs. The magnitude of number size distributions were similar for all the test samples, except for the fact that 4% CNTs generated more particles than any other test samples at each particle diameter, which was in accordance with the number concentration boxplots. In terms of the particle mass size distribution, a single mode was observed for all the test samples, with the peak at around 5 μm and the mass concentration ranging from 0.5 mg/m^3 to 1.8 mg/m^3. The mode was shifted to smaller diameter for 4% CNTs and to larger diameter for 0% CNTs compared to other percentages. Particles larger than 1 μm accounted for most of the mass size distribution. During sanding processes, 0% CNTs and 4% CNTs generated the greatest mass concentration at the peak, whereas 3% CNTs generated the least mass concentration.

Comparison of particle emissions for sanding speed

The results from test runs at various disc speeds are presented in Figure 4. The disc speed greatly determined both the number concentration and the respirable mass concentration (Panel (a) and (b) of Figure 4). The test operated at the fast disc speed produced a mean of 3100 particles/cm^3, 30 times of the mean concentration at the slow disc speed and 10 times of that at the medium disc speed. The difference in the mean of the number concentration and respirable mass concentration from the three disc sander speeds were statistically significant (Tukey's multiple comparison, $p<0.001$), as illustrated in Table 2 and Table 3. The variability in particle number concentration at the fast sanding speed was also the highest, ranging from 2190 particles/cm^3 to 4400 particles/cm^3. The respirable mass concentration corresponded to the disc speed as well, with the mean ranged from 0.12 mg/m^3 at the slow speed to 0.30 mg/m^3 at the fast speed.

No obvious peak was observed at the slow and the medium speed in the particle size number distribution as a function of particle size, as described in Panel (c) of Figure 4, indicating the particle size was homogeneous at these two speeds. However, the fast sanding speed generated particles predominantly smaller than 50 nm. The particle mass size distribution in Panel (d) of Figure 4 illustrates a peak at the particle diameter between 1 μm and 10 μm for all three disc speeds, while the magnitude was the greatest at the fast speed of more than 1.2 mg/m^3, followed by 0.9 mg/m^3 at the medium speed.

Comparison of particle emissions for sandpaper grit

Tests conducted with different sandpaper grit are summarized in Figure 5. Shown in Panel (a) of Figure 5, the greatest particle number concentrations were produced by the coarse sandpaper compared to the medium and the fine sandpaper. The number

concentration for coarse grit averaged 4670 particles/cm^3 and ranged from 2380 particles/cm^3 to 7680 particles/cm^3, whereas the average were 332 particles/cm^3 and 214 particles/cm^3 for medium and the fine sandpaper, respectively. For both number concentration and respirable mass concentration, coarse sandpaper type produced particles significantly different from medium sandpaper and fine sandpaper (Tukey's multiple comparison, $P<0.001$), as shown in Table 2 and Table 3. From Panel (b) of Figure 5, the respirable mass concentrations also varied depending on the sandpaper grit, with the fine sandpaper grit the highest (0.431-0.634 mg/m^3) and medium sandpaper the lowest (0.125-0.213 mg/m^3). Surprisingly, the coarse sandpaper produced respirable mass concentration between the sandpapers with medium and fine grit, suggesting the respirable mass concentration did not necessarily correspond to the sandpaper grit.

The particle size distribution is illustrated in Panel (c) and (d) of Figure 5, where the coarse sandpaper accounted for most of the number concentration in the size range smaller than 50 nm, while in other size ranges there was no significant difference between sandpaper types. The number concentration decreased when the size increases for coarse sandpaper. The mass size distributions were similar for all the three sandpapers at diameter less than 1 μm, while fine sandpaper produced significantly larger mass of coarse particles. The mass distribution peaked at 7 μm with the respirable mass concentration of 3 mg/m^3 at the peak, three times of that for medium and fine sandpaper. It can be concluded that the fine sandpaper produced the highest number concentration at the nano size and mass concentration at the large size.

Comparison of particle emissions for different test samples

The number concentration and respirable mass concentrations were different according to test samples, as demonstrated in Panel (a) and (b) of Figure 6. The number concentration produced by Sample 2 outnumbered the other two samples and ranged from 858 particles/cm^3 to 2320 particles/cm^3, while there was a significant difference between 2% CNTs and Sample 1, which averaged 332 particles/cm^3 and 454 particles/cm^3, respectively. The number concentration range for both Sample 1 and Sample 2 were larger than 2% CNTs. On the other hand, the respirable mass concentration for all the three samples ranged from around 0.13 mg/m^3 to around 0.22 mg/m^3 and averaged 0.17 mg/m^3. From Table 2 and Table 3, the number concentration from different test sample were significantly different from each other, and the respirable mass concentration from Sample 1 was different from Sample 2 and 2% CNTs (Tukey's multiple comparison, $p<0.001$). Panel (c) and (d) of Figure 6 showed the particle size distribution. There was a difference of number size distribution at the sizes smaller than 100 nm, with the Sample 2 generating the most and 2% CNTs generating the least number of particles; however the size distribution was almost the same in the above 1 μm particle size range. The particle size mass distribution for the three test samples were similar except for the fact that 2% CNTs peaked around 10 μm and the magnitude was 1.0 mg/m^3. The mass concentration was dominated by particles with the size larger than 1 μm, while particles less than 1 μm were negligible.

Particle emission when the disc sander is on but the feed is off

The particle number concentration was 100 particles/cm^3 at the beginning of the test and dropped below 80 particles/cm^3 over time. The respirable mass concentration corresponded to the number concentration, numbering 0.2 mg/m^3 when the tests started and dropped below 0.005 mg/m^3 later. The particle size distribution shows a particle number of 30 particles/cm^3 in the nano-size range, diminished to almost 0 particles/cm^3 at the larger particle size and increased back above 10 particles/cm^3 at the largest size detectable by SMPS. The result showed a negligible amount of particles generated when the test sample was not fed to the spinning disc sander.

Microscopy analysis results

The images of airborne particle samples taken with SEM and TEM were presented in Figure 7. CNT protrusions with outer diameter of 50 nm were found sticking out of the particle surface.

Discussion

The study simulated a typical life cycle event of sanding. An association of particle generation and test conditions was found. Particle number and respirable mass concentrations were measured with different CNTs percentage under different sanding conditions. Contrary to Wohlleben et al. (2011), the particle release was a continuous process. The number concentrations had a poly disperse curve, and the peak varied by composite type, which was supported by Bello et al. (2008). For different test samples, the highest particle number concentrations were produced with test samples composed of 4% CNTs, and the number concentration was doubled compared to 1% CNTs. Similarly,

respirable mass concentrations produced with the 4% CNTs test samples were 0.35 mg/m^3, which were three times higher than the concentrations produced by 0%, 1%, and 3% CNTs test samples, as illustrated in the boxplots. The particle mass size distribution also showed that 4% CNTs generated the greatest amount of respirable mass concentration. From the test results, we conclude that for a given mechanical energy input, a greater fraction of CNTs in the test samples increases the nano and respirable size particles. One speculation is that the presence of CNTs makes the epoxy test sample more brittle and easier to break into small particles during sanding process. This notion is similar to that proposed by Göhler et al. (2010) and Wohlleben et al. (2011) who suggested that the rigidity of the test samples rather than the presence of nano-additives determined the particle concentration. A mechanical study found that tensile strength of the composite filled with well dispersed CNTs increases (Song & Youn, 2005), which helps to explain the sanding test results.

Changes in the disc sander speed resulted in differences in number and respirable mass concentrations. The slowest speed applied in the test produced particle number comparable to the background concentration, whereas the fast disc speed produced more than 30-fold number concentration compared to background. The respirable mass concentrations corresponded to the disc speed as well, and all concentrations were significantly higher than background concentrations. This fact could be explained by the increased abrasion energy to break up the test samples induced by increased disc speed. The source for nano-sized and respirable sized particles could either be the burning of the sandpaper adhesive backing due to the heat generated from abrasion or the nanoparticles in CNTs test samples, and further microscopy studies should be done to look at the

morphology of airborne particles. Tests were performed when the disc sander with sandpaper on it was spinning but no test samples were fed to the disc, and the result showed that little nano sized particles were generated. Thus, the burning may originate from the friction of test samples and sandpaper rather than the spinning of disc sander, and the friction increased with disc sander speed.

Particle number and respirable mass concentrations were also associated with the grit of the sandpaper. The particles produced by coarse sandpaper averaged 4700 particles/cm^3, significantly higher than particles from medium and fine sandpaper. The finding was supported by Chung et al. (2000) that the finer grade paper generated less dust. Our study showed that fine grit sandpaper produced the highest respirable mass concentration on the other hand. The finding that the size of the observed number concentration modes are most likely to depend on factors such as sandpaper grit size and the sander engine rotation speed is in agreement with Koponen et al. (2009). In terms of varying the test samples, the three test samples produced respirable mass concentration ranging from 0.13 mg/m^3 to around 0.22 mg/m^3, whereas Sample 2 produced number concentration 1500 particles/cm^3 in average, which was three times higher than that of 2% CNTs and Sample 1.

The overall shape of the particle mass distribution produced from sanding test samples remained similar, regardless of test conditions. For all particle mass size distribution, a mode was observed from 1 μm to 10 μm, and the magnitude varied depending on mechanical energy (fast speed > medium speed >slow speed) and sandpaper grit (coarse>medium and fine).In contrast, substantial differences were observed in the particle number size distributions produced under different test objects

and generation parameters. For instance, for test samples with different CNTs percentage, the particle size distributions were different in terms of the particle size at the peak and the magnitude of the peak; generally there were two modes at the number size distribution curve, one at around 1 μm in diameter and the other one at around 100 nm in diameter. The one at around 1 μm corresponds to the mode on the mass size distribution, while the other mode at smaller than 100 nm corresponds to respirable mass concentration at nano size which is negligible in the particle mass size distribution, partly because particles with small diameter accounts for less mass.

Further, the source of the particles may be attributed to the mechanical breakage of the test samples, the heat generated from the back of the sandpaper, and the wearing of sandpaper grit. Typically, the particles generated from mechanical breakage are larger than 0.5 μm (Hinds, 1998), which corresponded to the mode in the particle size distribution. The high number concentration at nano size is speculated to be the burning of sandpaper back under certain test conditions. A justification for the speculation is for a specific disc sander speed, 4% CNTs has the highest tendency to break into particles, which suggests the most energy in sanding and thus the most amount of heat and burning, and it corresponds to the fact that 4% CNTs produced the highest number concentration less than 100 nm. This speculation could also explain the particles sized less than 50 nm, which dominate the number size distribution for particles generated in fast disc speed. Koponen (2009) also found that the sander was the main source of particles smaller than 50 nm. The particles produced could be partly attributed to the sandpaper grit as well, since the wearing of sandpaper was found in the 12-minute

sanding tests, which is in contradiction with Gohler et al. (2010). Wohlleben et al. (2011) also considered sandpaper as a source of particles.

Regarding to the microscopy analysis, an explanation of the protrusion is that since CNTs have higher rigidity than epoxy, they are less prone to break and tend to stick out of the surface of epoxy. Similar to Cena & Peters (2011), Vorbau et al. (2009), and Göhler et al. (2010)'s findings, no free CNTs were found in microscopic analysis. Also, the morphology of the particles generated during sanding was different from CNTs-incorporating bulk material.

From a regulatory perspective, the respirable mass concentrations produced by all the test samples were considerably lower than the OSHA PEL for PNOR of 15 mg/m^3 and ACGIH respirable particle PNOS TLV of 3000 $\mu g/m^3$. However, one should keep in mind that there is no specific standard regulating CNTs-epoxy nanomaterials.

Conclusion

An association of particle generation and test conditions was found. The determinants of particle concentration include the brittleness of test samples and the abrasion energy, which is associated with sandpaper grit and disc speed during sanding process. In addition to the abrasion, the friction originated by the contact of test samples and sandpaper may cause the sandpaper adhesive backing to burn, thus generating nano-sized and respirable sized particles.

This study presented a well-defined test apparatus and standardized method to characterize the particle emission during sanding process, and a high repeatability was achieved with both CNTs-composites and selected commercial products. Also the methodologies established could be modified for any other nanocomposite products and

extended to other life cycle events such as exposure to sunlight. Future studies on the inhalation toxicity of environmentally-relevant aerosols could be accomplished with the combination of the test apparatus and a toxicological test chamber.

There are several limitations for this study that required attention. The combination of the OPC data and the SMPS data might not accurately reflect the particle size distribution since the two measurements are based on the optical and electric properties of particles, respectively. Moreover, this study failed to adjust the refractive index of particles produced from different test samples; the fact that the test samples have different colors leads to an inconsistency of refractive index. Further, the agglomeration of dusts originated from nanocomposites sanding materials in the exhaust may also affect the measurement of particle number concentration. The density of all test samples is assumed to be 1 g/cm^3, lower than the density of pure epoxy of 1.19 g/cm^3 and the density of pure MWCNTs of 1.8-2.0 g/cm^3, and the difference may affect the comparability of mass concentration with other studies. Plus, the difference in the particle release ability of different test samples may not be safely explained due to the lack of brittleness test of all the test samples and commercial products. Finally, microscopy analysis data we have are insufficient to explain for the nano-sized particles produced with coarse sandpaper and particles produced at fast sanding speed.

Test Sample	Sandpaper Type			Disc Sander Speed	
CNTs Percentage, % or Sample Name	Roughness	Grit Level	Presenting Grit Size, μm	Speed	RPM
0	Medium	P150	100	Medium	1425
1	Medium	P150	100	Medium	1425
2	Medium	P150	100	Medium	1425
3	Medium	P150	100	Medium	1425
4	Medium	P150	100	Medium	1425
Sample 1	Medium	P150	100	Medium	1425
Sample 2	Medium	P150	100	Medium	1425
2	Coarse	P80	201	Medium	1425
2	Fine	P320	46.1	Medium	1425
2	Medium	P150	100	Fast	2167
2	Medium	P150	100	Slow	586

Table 1. Test conditions.

Test Condition	Number of Samples	Number Concentration Mean, particles/cm^3 (SD)	Grouping
CNTs Percentage (%)			
4	3	455 (99)	**A**
0	3	361 (80)	**A B**
3	3	340 (91)	**B C**
2	3	332 (55)	**C**
1	3	200 (82)	**D**
Disc Sander Speed			
Fast	3	3140 (581)	**A**
Medium	3	332 (55)	**B**
Slow	3	92 (18)	**C**
Sandpaper Type			
Coarse	3	4670 (1220)	**A**
Medium	3	332 (55)	**B**
Fine	3	214 (124)	**B**
Test Sample			
Sample 2	3	1470 (397)	**A**
Sample 1	3	454 (204)	**B**
2% CNTs	3	332 (55)	**C**

Table 2. Comparison of number concentration mean between different test conditions using one-way ANOVA and multiple comparison with Tukey's test at alpha=0.05. $P<0.001$

Test Condition	Number of Samples	Respirable Mass Concentration Mean, mg/m^3 (SD)	Grouping
CNTs Percentage (%)			
4	3	0.348 (0.05)	**A**
2	3	0.173 (0.02)	**B**
0	3	0.132 (0.02)	**C**
1	3	0.129 (0.02)	**C**
3	3	0.125 (0.03)	**C**
Disc Sander Speed			
Fast	3	0.298 (0.03)	**A**
Medium	3	0.173 (0.02)	**B**
Slow	3	0.117 (0.01)	**C**
Sandpaper Type			
Fine	3	0.557 (0.04)	**A**
Coarse	3	0.208 (0.03)	**B**
Medium	3	0.173 (0.02)	**B**
Test Samples			
Sample 1	3	0.184 (0.02)	**A**
2% CNTs	3	0.173 (0.02)	**B**
Sample 2	3	0.170 (0.02)	**B**

Table 3. Comparison of respirable mass concentration mean between different test conditions using one-way ANOVA and multiple comparison with Tukey's test at alpha=0.05. $P<0.001$

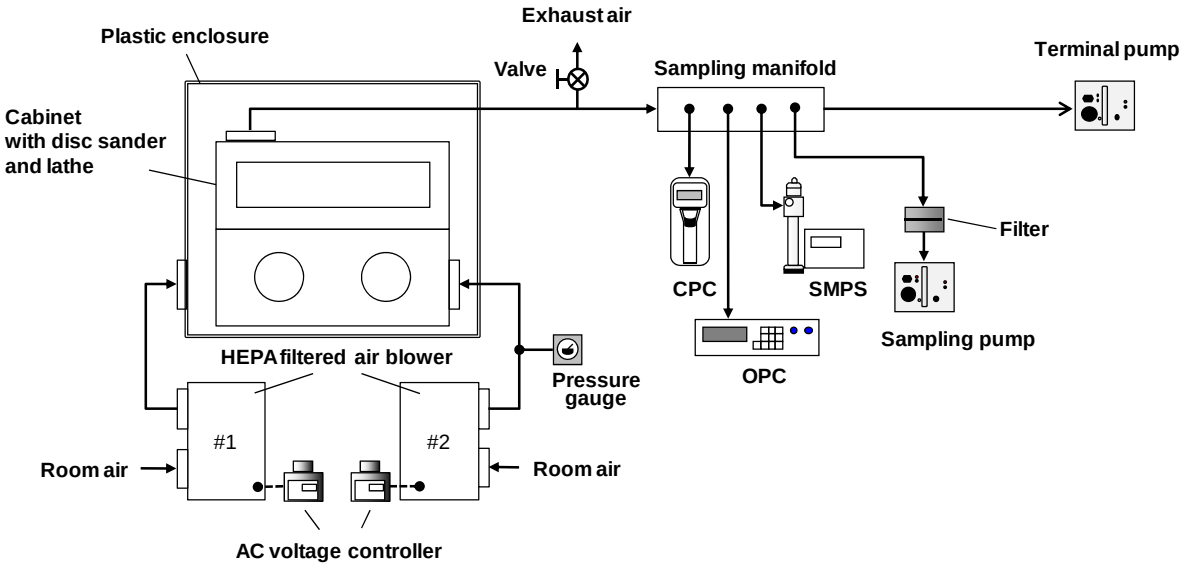

Figure 1. Experimental setup.

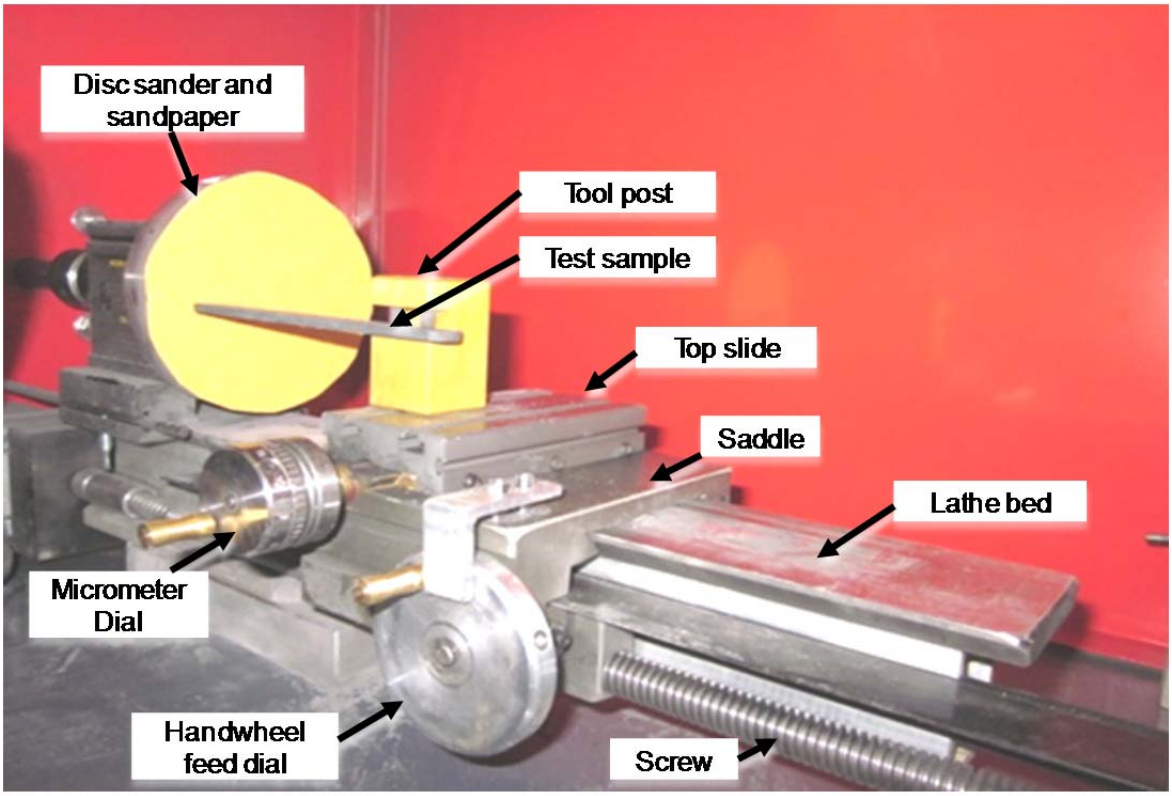

Figure 2. Disc sander and lathe.

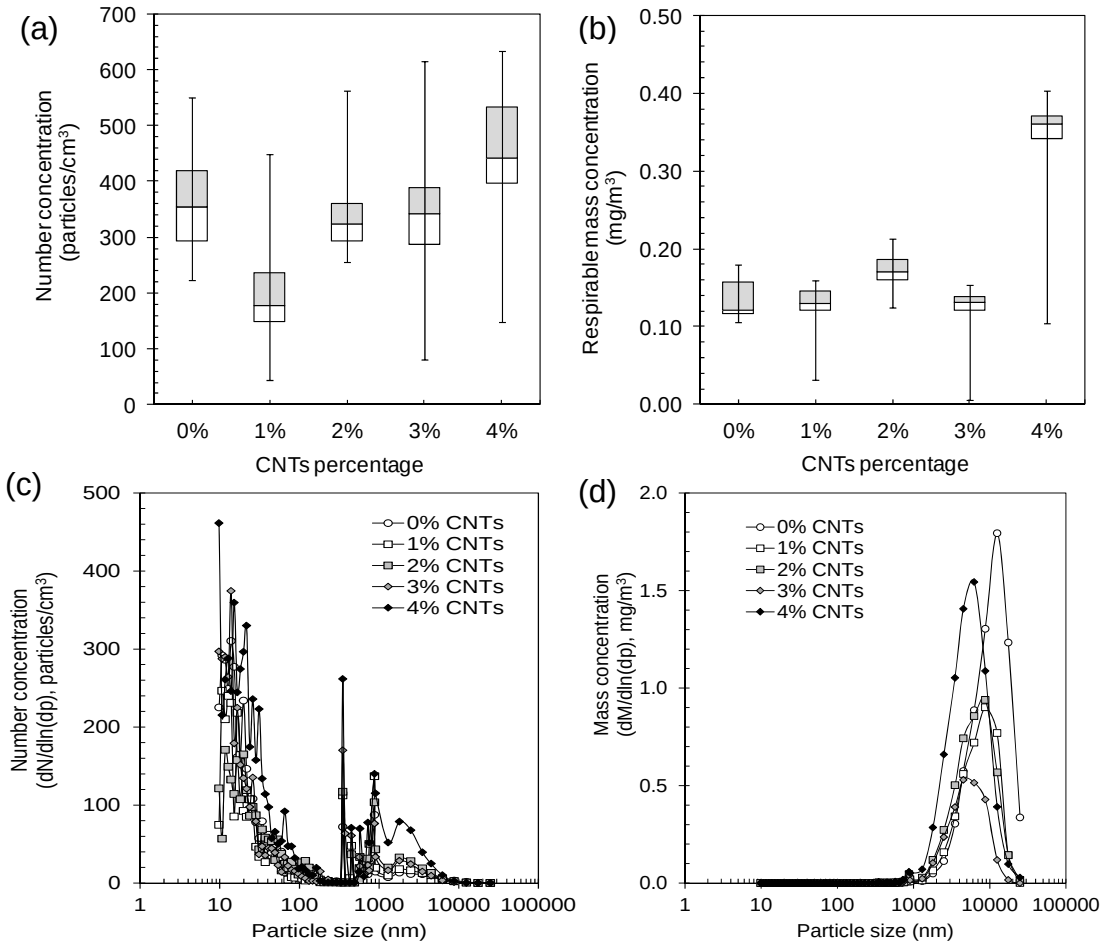

Figure 3. Boxplots of (a) number concentration and (b) respirable mass concentration and particle size distribution of (c) number and (d) mass for percentages of CNTs when using the medium disc sander and the medium sandpaper grit.

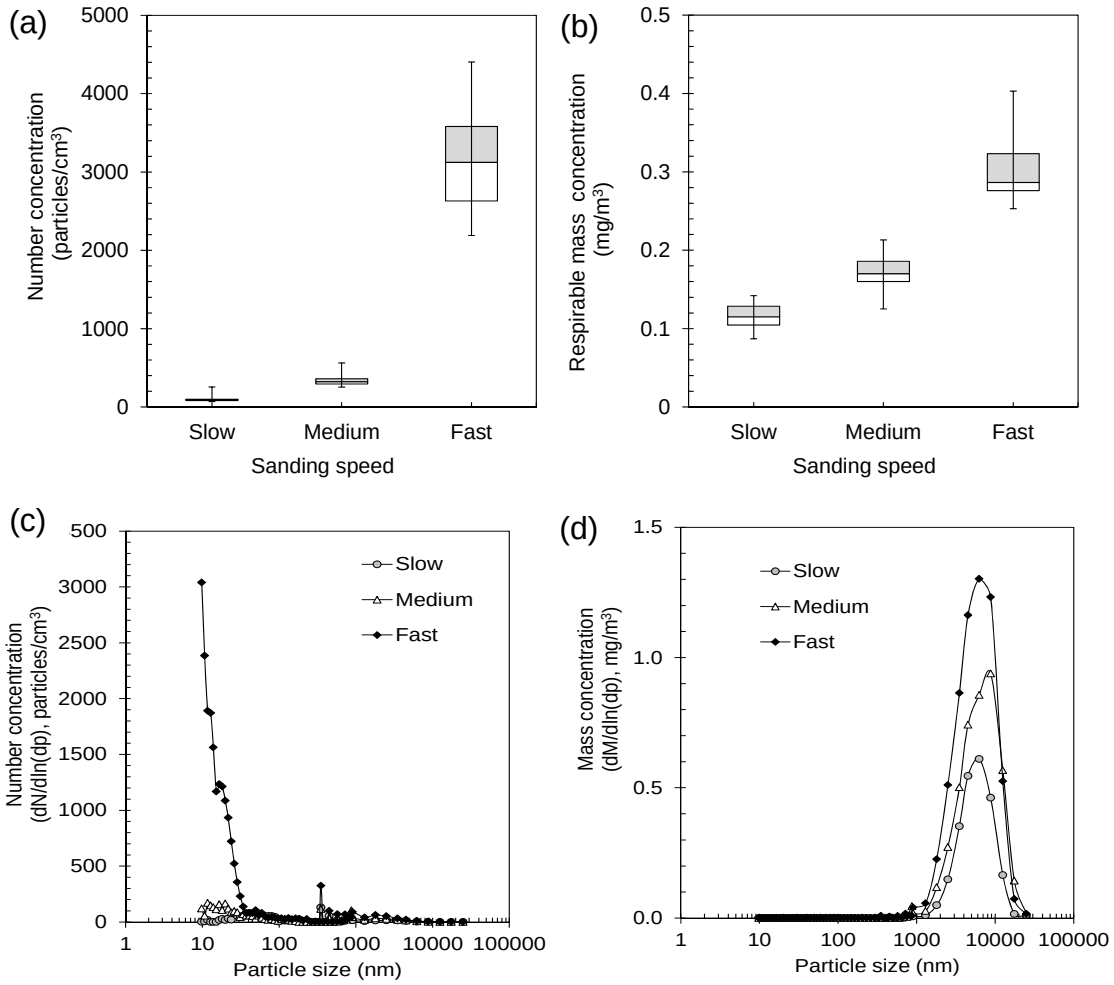

Figure 4. Boxplots of (a) number concentration and (b) respirable mass concentration and particle size distribution of (c) number and (d) mass for sanding disc speed when using the 2% CNTs test sample and the medium sandpaper grit.

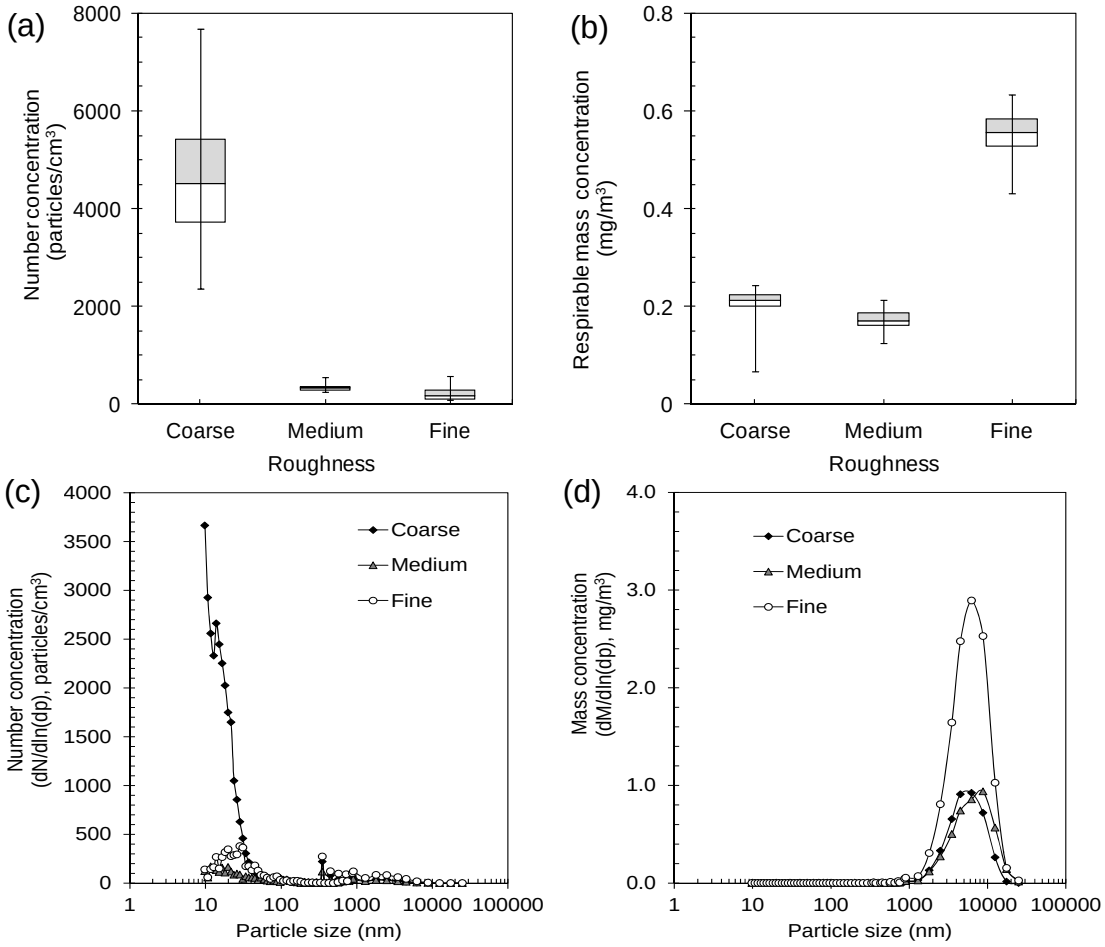

Figure 5. Boxplots of (a) number concentration and (b) respirable mass concentration and particle size distribution of (c) number and (d) mass for roughness of sandpaper when using the 2% CNTs test sample and the medium disc sander speed.

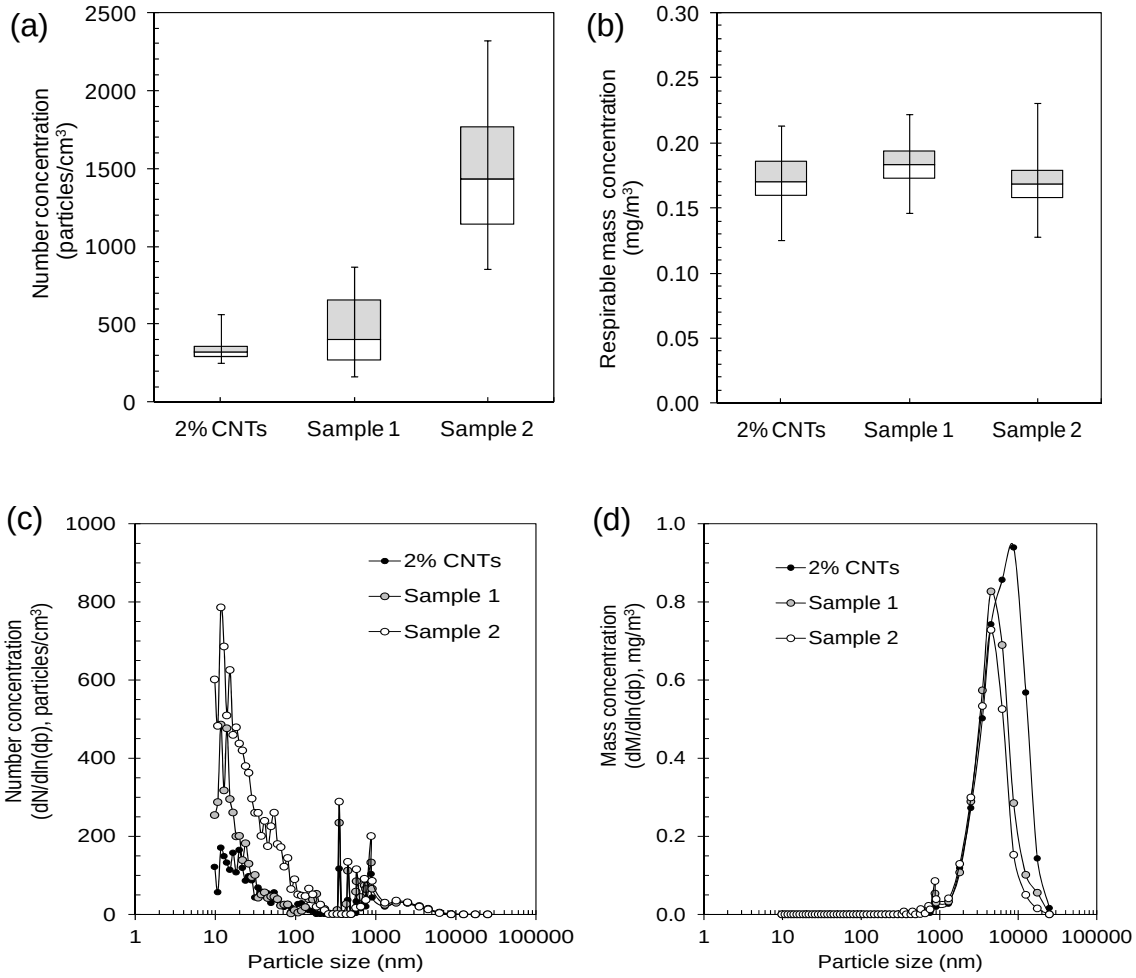

Figure 6. Boxplots of (a) number concentration and (b) respirable mass concentration and particle size distribution of (c) number and (d) mass for different test samples when using the medium disc sander speed and the medium sandpaper grit.

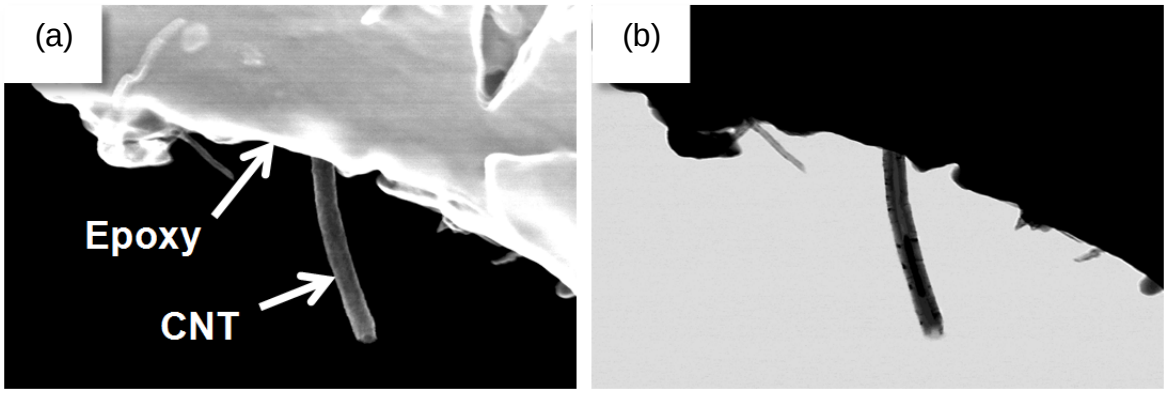

Figure 7. Microscopy images including (a) SEM image and (b) TEM image of 2% CNTs-epoxy nanocomposite particle.

CHAPTER 3 CONCLUSION

The magnitude of the emitted particles in various nanocomposite LCAs including sanding has been a concern especially during workplace exposure, and the potential health effects of the particles are unknown. Methods are available to assess the particle release during different processes, but most of them are not well standardized.

In this study, a well-defined test apparatus and standardized method was developed to characterize the particle release during sanding of CNTs-composites and commercial products. The property of particle emission was assessed with number concentrations, respirable mass concentrations and particle number/mass size distribution. The morphology of particles for selected samples was assessed through the microscopy analysis of airborne particle samples.

A great magnitude of particle release was observed when the disc sander and the carriage were activated. Also, the difference of particle release was found under different test conditions including sanding disc speed, sandpaper grit size, and test sample type. Further analysis showed that the variation of the abrasion energy could be a cause for the difference in particle release, and the heat on the back of the sandpaper generated through disc sander rotation from the contact of the sandpaper and test sample can be another cause of particle emission. . During microscopy analysis, embedded CNTs protrusions were observed extending outward beyond the outside of particles. This study suggests a potential generation of particles during the life cycle event of sanding, whereas the particle concentrations are below current health-based limits on mass metrics proposed by OSHA and ACGIH.

Further test should include brittleness test of all the test samples and commercial products to verify the particle release ability. Microscopy and elemental analysis should be carried out to verify the source of nano-sized particles produced with coarse sandpaper and particles produced at fast sanding speed. Future tests simulating other life-cycle events under conditions such as sunlight should be performed to reveal the particle release under other conditions, and the test protocol developed in this test could be applied to ensure the repeatability and comparability. A toxicological test chamber was also reserved for future use to study the inhalation toxicity of airborne particles produced.

REFERENCES

ACGIH®: 2011 TLVs and BEIs. Cincinnati, Ohio: ACGIH, 2011.

Ajayan, P. A. & Zhou, O. Z. (2001). Applications of carbon nanotubes, *Topics in Applied Physics, 80,* 391-425.

Ando, Y., Zhao, X., Sugai, T., & Kumar, M. (2004). Growing carbon nanotubes. *Materials Today, 7(10),* 22-29.

Bello, D, Wardle, B. L., Zhang, J., Yamamoto, N., Santeufemio, C., Hallock, M., & Virji, M. A. (2010). Characterization of exposures to nanoscale particles and fibers during solid core drilling of hybrid carbon nanotube advanced composites. *International Journal of Occupational* and *Environmental Health*, *16(4),* 434-450.

Bhatti, P., Newcomer, L., Onstad, L., Teschke, K., Camp, J., Morgan, M., & Vaughan, T. L. (2011). Wood dust exposure and risk of lung cancer. *Occupational* and *Environmental Medicine*, *68(8),* 599-604.

Boutou-Kempf, O., Marchand, J., Radauceanu, A., Witschger, O., Imbernon, E., & the Group Health Risks of Nanotechnologies (2011). Development of a French epidemiological surveillance system of workers producing or handling engineered nanomaterials in the workplace. *Journal of Occupational and Environmental Medicine, 53(6),* 103-107.

Cena, L. G. & Peters, T. M. (2011). Characterization and control of airborne particles emitted during production of epoxy/carbon nanotube nanocomposites. *Journal of Occupational and Environmental Hygiene, 8(2),* 86-92.

Chung, K. Y. K., Cuthbert, R. J., Revell, G. S., Wassel, S. G., & Summers, N. (2000). A Study on Dust Emission, Particulate Size Distribution and Formaldehyde Concentration during Machining of Medium Density Fiberboard. *The Annals of Occupational Hygiene, 44(6),* 455–466.

Dahm, M. M., Yencken, M. S., & Schubauer-Berigan, M. K. (2011). Exposure control strategies in the carbonaceous nanomaterial industry. *Journal of Occupational and Environmental Medicine, 53(6),* 68-73.

David, R. M., Nasterlack, M., Engel, S., & Conner, P. R. (2011). Developing a registry of workers involved in nanotechnology: BASF experiences. *Journal of Occupational and Environmental Medicine, 53(6),* 32-34.

Decker, P., Cohen, B., Butala, J. H., & Gordon, T. (2002). Exposure to wood dust and heavy metals in workers using CCA pressure-treated wood. *American Industrial Hygiene Association Journal, 63(2),* 166-171.

Donaldson, K., Aitken, R., Tran, L., Stone, V., Duffin, R., Forrest, G., & Alexander, A. (2006). Carbon nanotubes: A review of their properties in relation to pulmonary toxicology and workplace safety. *Toxicological Sciences, 92(1),* 5-22.

EPA, Toxic Substances Control Act Inventory Status of Carbon Nanotubes, in Federal Register, 2008.

Göhler, D., Stintz, M., Hillemann, L., & Vorbau, M. (2010). Characterization of nanoparticle release from surface coatings by the simulation of a sanding process. *The Annals of Occupational Hygiene, 54 (6),* 615-624.

Hinds, W. C. (1998). Aerosol technology: properties, behavior, and measurement of airborne particles. New York, NY: Wiley-Interscience.

Hsu, L. Y. & Chein, H. M. (2007). Evaluation of nanoparticle emission for TiO_2 nanopowder coating materials. *Journal of Nanoparticle Research, 9(1),* 157-163.

Hubbs, A. F., Mercer, R. R., Benkovic, S. A., Harkema, J., Sriram, K., Schwegler-Berry, D., … Sargent L. M. (2011). Nanotoxicology—A pathologist's perspective. *Toxicologic Pathology, 39(2),* 301-324.

Hunt, R. & Frankli, W. E. (1996). LCA- How it came about- Personal reflections on the origin and LCA in the USA. *The International Journal of Life Cycle Assessment, 1(1),* 4-7.

Iijima, S. (1991). Helical microtubules of graphitic carbon. *Nature, 354(6348),* 56-58. Available at http://nanogloss.com/nanotubes/how-much-do-nanotubes-cost/#axzz1kboovmdJ

ISO, Workplace atmospheres—Ultrafine, nanoparticle, and nano-structured aerosols exposure characterization and assessment, 2007, ISO/TR 27628:2007, Geneva, Switzerland.

Köhler, A., Som, C., Helland, A., & Gottschalk, F. (2008). Studying the potential release of carbon nanotubes throughout the application life cycle source. *Journal of Cleaner Production, 16(8-9),* 927-937.

Koponen, I. K., Jensen, K. A., & Schneider, T. (2009). Sanding dust from nanoparticle-containing paints: Physical characterization. *Journal of Physics: Conference Series, 151,* 1-9.

Kroto, H. W., Heath, J. R., O'Brien, S. C., Curl, R. F., & Smalley, R. E. (1985). C_{60}: Buckminsterfullerene. *Chemical Reviews, 91(6),* 1213-1235.

Kuempel, E. D. (2011). Carbon nanotube risk assessment implications for exposure and medical monitoring. *Journal of Occupational and Environmental Medicine, 53(6),* 91-97.

LeBlanc, A. J., Moseley, A. M., Chen, B. T., Frazer, D., Castranova, V., & Nurkiewicz, T. R. (2010). Nanoparticle inhalation impairs coronary microvascular reactivity via a local reactive oxygen species-dependent mechanism. *Cardiovascular Toxicology, 10(1),* 27-36.

Leonhardt, A. (2004). Synthesis of single-walled carbon nanotubes by CVD. Available at http://www.ifw-dresden.de/iff/13/research/swcnt/ and http://www.ifw-dresden.de/iff/13/research/swcnt/single wall cnt 1.htm.

Li, Z., Hulderman, T., Salmen, R., Chapman, R., Leonard, S. S., Young, S. H., …, Simeonova, P. P. (2007). Cardiovascular effects of pulmonary exposure to single-wall carbon nanotubes. *Environmental Health Perspectives, 115(3),* 377-382.

Ma-Hock, L., Treumann, S., Strauss, V., Brill, S., Luizi, F., Mertler, M., … Landsiedel, R. (2009). 134 TEEGUARDEN ET AL. Downloaded from http://toxsci.oxfordjournals.org/ at University of Iowa Libraries/Serials Acquisitions on February 1, 2012. Inhalation toxicity of multiwall carbon nanotubes in rats exposed for 3 months. *Toxicological Science, 112(2),* 468-481.

Mowat, F., Bono, M., Lee, R. J., Tamburello, S., & Paustenbach, D. (2005). Occupational exposure to airborne asbestos from phenolic molding material (bakelite) during sanding, drilling, and related activities. *Journal of Occupational and Environmental Hygiene, 2(10),* 497-507.

Mowat, F., Weildling, R., & Sheehan, P. (2007). Simulation tests to assess occupational exposure to airborne asbestos from asphalt-based roofing products. *The Annals of Occupational Hygiene, 51(5),* 451-462.

Muller, J., Huaux, F., Fonseca, A., Nagy, J. B., Moreau, N., Delos, M., … Fenoglio, I. (2008). Structural defects play a major role in the acute lung toxicity of multiwall carbon nanotubes: Toxicological aspects. *Chemical Research in Toxicology, 21(9),* 1698-1705.

Muller, J., Huaux, F., Moreau, N., Misson, P., Heilier, J. F., Delos, M., … , Lison, D. (2005). Respiratory toxicity of multi-wall carbon nanotubes. *Toxicology and Applied Pharmacology, 207(3),* 221-231.

National Nanotechnology Initiative (2011). *Environmental, Health, and Safety Research Strategy.*

NIOSH Current Intelligence Bulletin: Occupational Exposure to Carbon Nanotubes and Nanofibers. Available at

http://www.cdc.gov/niosh/docket/review/docket161a/pdfs/carbonNanotubeCIB_PublicReviewOfDraft.pdf

OSHA. Table Z-1 Limits for Air Contaminants (29 CFR 1910.1000 Z-1 Table); 2006.

OSHA. Table Z-1 Limits for Air Contaminants (29 CFR 1910.1000 Z-1 Table); 2011.

Paustenbach, D. J., Sage, A., Bono, M., & Mowat, F. (2004). Occupational exposure to airborne asbestos from coatings, mastics, and adhesives. *Journal of Exposure Analysis and Environmental Epidemiology, 14,* 234-244.

Peters, A., Ruckerl, R., & Cyrys, J. (2011). Lessons from air pollution epidemiology for studies of engineered nanomaterials. *Journal of Occupational and Environmental Medicine, 53(6),* 8-13.

Peters, T. M., Heitbrink, W. A., Evans, D. E., Slavin, T. J., & Maynard, A. D. (2006) The mapping of fine and ultrafine particle concentrations in engine machining and assembly plant. *The Annals of Occupational Hygiene, 50,* 249-257.

Pongratz, S. (2005). Die alterung von thermoplasten [The ageing of thermoplastic]. Alexander-universita¨t erlangen-Nürnberg.

Raynor, P. C., Cebula, J. I, Spangenberger, J. S., Olson, B. A., Dasch, J. M., & D′Arcy, J. B. (2012). Assessing Potential Nanoparticle Release During Nanocomposite Shredding Using Direct-Reading Instruments. *Journal of Occupational and Environemental Hygiene, 9(1),* 1-13.

Sargent, L. M., Hubbs, A. F., Young, S. H., Kashon, M. L., Dinu, C. Z., Salisbury, J. L., … Reynolds, S. H.(2011). Single-walled carbon nanotube-induced mitotic disruption. *Mutation Research: Genetic Toxicology and Environmental Mutagenesis,* doi:10.1016/j.mrgentox.2011.11.017.

Scheeper, B., Kromhout, H., & Boleij, J. S. (1995). Wood-dust exposure during wood-working processes. *The Annuals of Occupational Hygiene, 39 (2),* 141-154.

Schlünssen, V., Jacobsen, G., Erlandsen, M., Mikkelsen, A. B., Inger Schaumburg, I., & Sigsgaard, T. (2008). Determinants of wood dust exposure in the Danish furniture industry—Results from two cross-sectional studies 6 years apart, *The Annals of Occupational Hygiene, 52(4),* 227-238.

Schubauer-Berigan, M. K., Dahm, M. M., & Yencken M. S. (2011). Engineered carbonaceous nanomaterials manufacturers in the United States: Workforce size, characteristics, and feasibility of epidemiologic studies. *Journal of Occupational and Environmental Medicine, 53(6),* 62-67.

Shatkin, J. A. (2008). Nanotechnology Health and Environmental Risks. Taylor and Francis. Boca Raton, Florida.

Shvedova, A. A., Kisin, E. R., Mercer, R., Murray, A. R., Johnson, V. J., Potapovich, A. I., … Baron, P. (2005). Unusual inflammatory and fibrogenic pulmonary responses to single-walled carbon nanotubes in mice. *American Journal of Physiology - Lung Cellular and Molecular Physiology, 289(5),* 698-708.

Shvedova, A. A., Kisin, E. R., Murray, A. R., Gorelik, O., Arepalli, S., Castranova, V., … Oury, T. D. (2007). Vitamin E deficiency enhances pulmonary inflammatory response and oxidative stress induced by single-walled carbon nanotubes in C57BL/6 mice. *Toxicology and Applied Pharmacology, 221(3),* 339-348.

Shvedova, A. A., Kisin, E., Murray, A. R., Johnson, V. J., Gorelik, O., Arepalli, S., … Kagan, V. E. (2008). Inhalation vs. aspiration of single-walled carbon nanotubes in C57BL/6 mice: inflammation, fibrosis, oxidative stress, and mutagenesis. *American Journal of Physiology - Lung Cellular and Molecular Physiology, 295,* 552-565.

Smalley, R. E. (1991). Nanotechnology. Prepared written statement and supplemental material of R. E. Smalley, Rice University, June 22, 1999. In *U.S. House of Representatives Committee on Science, Basic Research Subcommittee Hearings*, U.S. Government, Washington, DC.

Song, Y. S. & Youn, J. R. (2005). Influence of dispersion states of carbon nanotubes on physical properties of epoxy nanocomposites. *Carbon, 43 (7),* 1378–1385.

Tabet, L., Bussy, C., Setyan, A., Simon-Deckers, A., Rossi, M. J., Boczkowski, J., & Lanone, S. (2011). Coating carbon nanotubes with a polystyrene-based polymer protects against pulmonary toxicity. *Particle and Fibre Toxicology, 21, 8(3).* doi:10.1186/1743-8977-8-3.

Teeguarden, J. G., Webb-Robertson, B. J., Waters, K. M., Murray, A. R., Kisin, E. R., Varnum, S. M., … Shvedova, A. A. (2011). Comparative proteomics and pulmonary toxicity of instilled single-walled carbon nanotubes, crocidolite asbestos, and ultrafine carbon black in mice. *Toxicological Science, 120(1),* 123-135.

The Food and Environment Research Agency (FERA) (2009). Nanolifecycle—A lifecycle assessment study of the route and extent of human exposure via inhalation for commercially available products and applications containing carbon nanotubes. York, the United Kingdom: Chaudhry, Q., Aitken, R., Hankin, S., Donaldson, K., Olsen, S., Boxall, A., Kinloch, I., Friedrichs, S.

Thorpe, A., & Brown, R. C. (1994). Measurements of the effectiveness of dust extraction systems of hand sanders used on wood. *The Annuals of Occupational Hygiene, 38(3),* 279-302.

Tsai, S. J., Ada, E., Isaacs, J. A., & Ellenbecker, M. J. (2009). Airborne nanoparticle exposures associated with the manual handling of nanoalumina and nanosilver in fume hoods. *Journal of Nanoparticle Research, 11(1),* 147-161.

Tsai, S., Hoffmann, M., Hallock, M., Ada, E., Kong, J., & Ellenbecker, M. (2009). Characterization and evaluation of nanoparticle release during the synthesis of single-walled and multiwalled carbon nanotubes by chemical vapor deposition. *Environmental Science and Technology, 43(15),* 6017-6023.

Verma, D. K. & Middleton, C. G. (1980). Occupational exposure to asbestos in the drywall taping process. *American Industrial Hygiene Association Journal, 41(4),* 264-269.

Vorbau, M., Hillemann, L., & Stintz, M. (2009). Method for the characterization of the abrasion induced nanoparticle release into air from surface coatings. *Aerosol Science, 40(3),* 209 - 217.

Warheit, D. B., Borm, P. J., Hennes, C., & Lademann, J. (2007). Testing strategies to establish the safety of nanomaterials: Conclusions of an ECETOC workshop. *Inhalation Toxicology, 19(8),* 631-643.

Welling, I., Lehtimäki, M., Rautio, S., Lähde, T., Enbom, S., Hynynen, P., & Hämeri, K. (2008). Wood dust particle and mass concentrations and filtration efficiency in sanding of wood materials. *Journal of Occupational and Environmental Hygiene, 6(2),* 90-98.

Wohlleben, W., Brill, S., Meier, M. W., Mertler, M., Cox, G., Hirth, S.,… , Robert Landsiedel, R. (2011). On the lifecycle of nanocomposites: Comparing released fragments and their in-vivo hazards from three release mechanisms and four nanocomposites. *Small, 7(16),* 2384-2395.

APPENDIX A TEST PROTOCOL

Purpose and Applicability

This document outlines a procedure to set up and operate a sand blasting cabinet. This cabinet is used to assess the release of engineered nanomaterial from commercial products during typical life-cycle events. Also described are procedures to troubleshoot potential problems when operating the cabinet.

Safety and Operating Precautions

All sharp hardware (e.g., screws) is to be disposed in appropriate place. Always wear goggles, N95 respirator, gloves, and disposable laboratory coat when setting up, reprogramming, and operating the cabinet. Make sure that equipment (e.g., pulley) which could potentially cause trauma remains in good shape.

Apparatus setup

Figure 1 in the main text describes the schematic diagram of the apparatus setup. The sand blasting cabinet is the red chamber pictured below. Basically how it works is that the cabinet houses a disc sander, which breaks test samples into particles. A lathe feeds the test sample toward the disc sander. The HEPA filtered air is pulled in both the cabinet and the plastic enclosure outside with two air movers, goes through a sampling manifold connecting to the direct reading instruments, and pulled out by the terminal pump.

The plastic enclosure is supported by PVC pipes and designed in order to isolate the cabinet from background air. The enclosure should be remained in a positive pressure, and the cabinet is kept in a slightly negative pressure.

Experimental system set up

a. Set up system according to the schematic diagram (Figure A1)

Figure A1. The setup of the whole system.

b. Set the disc sander speed

Adjust the position of the pulleys (to achieve 1425 RPM, set the motor pulley to the flange with the 4th largest diameter and the drive pulley to the flange with the 3rd largest diameter) (Figure A2)

Figure A2. The motor pulley and the drive pulley.

Figure A3. Rate set at 9.0.

c. Set the carriage speed

   i. Set the potentiometer to a specific value, which can be selected from Table A1

   ii. When reading /setting the potentiometer, align the fractional number with the middle of the box for full digit (Figure A3)

d. Install the test sample on the carriage

   i. Open the rear door of the cabinet

   ii. Insert the test sample into the gold holder with hex screws; align the sample at right angle to the disc sander, adjust the distance between the test sample and the outer edge of the disc sander to be 2.16 cm (Figure A4)

   iii. Close the rear door and lock the door

   iv. Move the test sample into position against the disc sander using the gloves

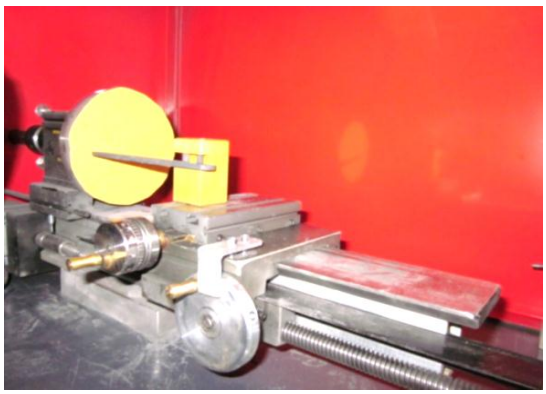

Figure A4. Test sample mounted on the carriage.

Airflow setup

a. Turn on both the air movers (Figure A5)

b. Perform visual/hand check for major leaks

c. Turn on the manometer, and adjust the exhaust valve to achieve a static pressure in the cabinet of -0.09 inch water gauge (''wg) to -0.11''wg (Figure A6)

d. Record the pressure drop for the cabinet supply air flow (magnehelic pressure gauge)

Figure A5. The air movers switched on.

Figure A6. The pressure inside the cabinet.

Data Collection System

a. Prepare the CPC
   i. Soak the CPC wick in isopropanol for 5 min and insert the wick into the CPC
   ii. Turn on the CPC and wait for warm up
   iii. Connect the zero filter to the CPC air inlet and verify the total particle count is less than 5 particles/cm^3)
b. Connect the CPC, OPC, and SMPS to the sampling manifold
c. Switch on the computer and the OPC
d. Set up the communications between the direct reading instrument and the computer
   i. Launch PRG Comm V1.1.1.0 program
   ii. Verify the CPC and OPC communication
   iii. Name a file with the date of test in the format of yyyymmdd.testi (i indicates the i^{th} test, e.g., 20110101.test1)
   iv. Start logging
   v. Press enter when asked for test location
   vi. In laboratory notebook, record the activity, the time for activity and CPC and OPC read
   vii. Switch on SMPS for warm-up

Run test

a. Before each test, connect the filter cassette with a new piece of filter to the cabinet

b. Measure the particle number concentration and respirable mass concentration when both the carriage and disc are off (5 minutes)
c. Measure emissions during sanding
   i. Set direction toggle switch to FWD
   ii. Set free-run toggle switch to RUN
   iii. Turn on the disc sander and carriage simultaneously
   iv. Start stop watch after the number concentration drops below 100 particles/cm^3 and respirable mass concentration is below 0.005 mg/m^3, wait for approximately 5.5 minutes until one SMPS run ends
   v. Turn on the sampling pump as soon as SMPS pops out a new run, sample at the flow rate of 1 LPM
   vi. Sample for approximately 6.5 minutes and turn off the sampling pump when the SMPS pops out a new run

After the test

a. Wearing N95 respirator, take a dust sample below the disc sander
b. Archive the sample in a labeled petri dish with the test conditions and date
c. Remove the sandpaper from the disc sander
d. Wearing N95 respirator, clean the remaining dust in the cabinet and then apply a vacuum

Trouble shooting and solutions

a. When CPC/OPC read is below normal values during sanding

i. Check whether the disc sander has stopped or not. If yes, turn on the light inside chamber or flash light to see if the spring is detached to the disc sander. Turn off the switch for the sander and carriage, screw the spring toward the disc manually when a disconnection occurs

ii. If the spring is still connected, backward the feed carriage until there is no contact between the sander and the test sample

iii. Turn the sander back on to see if it rotates

iv. If the disc rotates again, switch the carriage back on, push it toward the disc at the fastest carriage speed. Switch the free/run to free once the sample touches the disc, and switch the potentiometer back to the original place

v. Hit the free/run switch so that everything goes back to normal

b. When CPC/OPC number is extremely higher than normal during sanding Go around the whole apparatus to see if there is leakage. If no visible leak is observed, monitor number concentration with CPC first at conjunctions and then along the pipes. Fix the problem if leakage is detected.

Carriage speed overview

A description of the operation of the rate control may be beneficial in understanding. The potentiometer's wiper is connected to an 8-bit (2^8 = 256 counts) analog-to-digital converter (ADC). The ADC result is increased by a factor of 1.5 to achieve the desired range of travel rates. A constant of 2 is added to avoid stepping the motor faster than it is capable. This number is then doubled since the motor steps only on each low-going pulse. The resulting number is the time delay between steps in units of

milliseconds. The stepper motor rotates 1.8 degrees per step and there are 10 threads (or revolutions) per inch on the acme screw. The actual feed rate was measured and calculated by dividing the distance of feed by the duration of feed. Table A1 illustrates the number on the potentiometer and corresponding actual feed rate and Figure A7 plots the linear regression between the number and corresponding actual feed rate.

Number	Distance (inch)	Speed (minutes/inch)
end	2.03	0.164204
0	1.743	0.191241
0.1	0.564	0.591017
0.2	0.409	0.814996
0.3	0.324	1.028807
0.4	0.242	1.37741
0.5	0.211	1.579779
0.6	0.191	1.745201
0.7	0.175	1.904762
0.8	0.129	2.583979
0.9	0.122	2.73224
1	0.117	2.849003
2	0.081	4.115226
3	0.034	9.803922
4	0.038	8.77193
5	0.011	30.30303
6	0.025	13.33333
7	0.024	13.88889
8	0.02	16.66667
9	0.013	25.64103

Table A1.The numbers on the potentiometer related to the actual carriage speed.

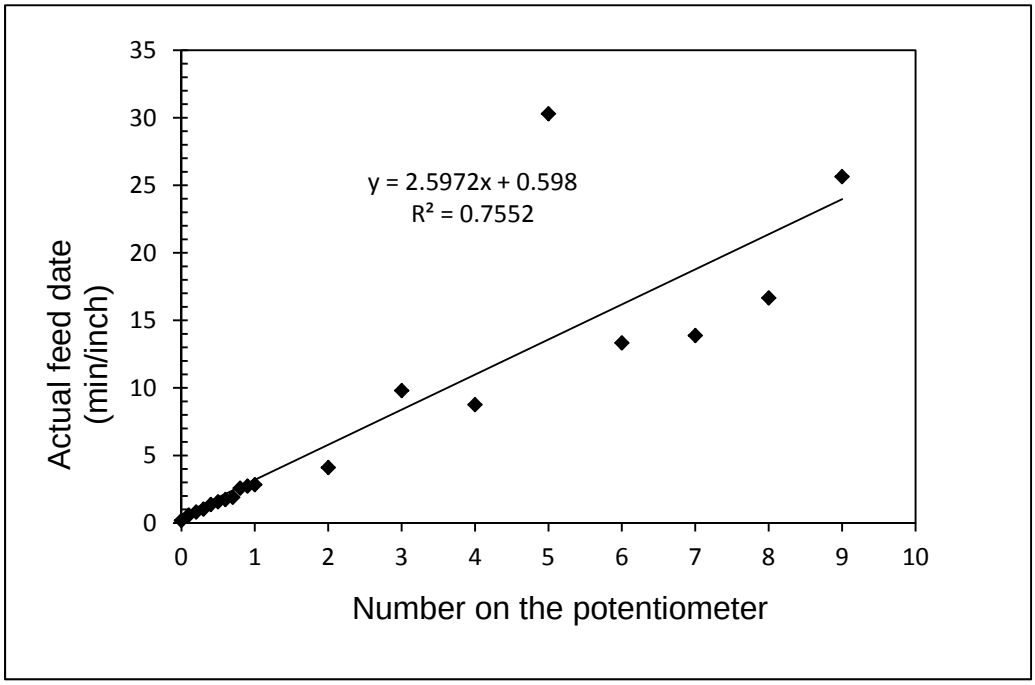

Figure A7. The linear regression between the number on the potentiometer and actual carriage speed.

Determination of disc sander speed

a. Apply an appropriately (0.5 inch) sized square piece of reflective tape to the surface of the disc, switch on the disc

b. Point the tachometer toward the disc at a distance of 2 inch to 20 inch

c. Press the Measure button (MEAS) on the tachometer and align the laser light beam with the reflective tape

d. Verify that the Monitor Indicator appears on the LCD when the reflective tape passes through the light beam

e. To change units (RPM or REV), release the MEAS button and press the MODE button.

f. When the Measure button is released, the last reading will remain in the display for 5 to 10 seconds before the Auto Power Off feature turns the meter off.

g. With the meter OFF, press the MEM (memory) button to recall the MAX, MIN and LAST rpm values or the last count (REV) from the last measurement period.

APPENDIX B PRECISION TEST

10 precision test runs were carried out in the standardized method at the medium sanding speed with sandpaper of medium roughness and 2% CNTs test samples. During the precision test, there was a variation in number concentration due to the limitations inherent in sanding disc and feed carriage, and the arithmetic mean ranged from 100 particles/cm^3 to 600 particles/cm^3. It turned out that respirable mass concentration was relatively stable both in one run over time and between different runs; the arithmetic mean ranges from 0.15-0.22 mg/m^3. However, there was one outlier in which the concentration was significantly lower than the others. The precision test results were consistent with the data obtained when sanding 2% CNTs under medium disc speed with medium sandpaper.

APPENDIX C THE MEAN OF NUMBER CONCENTRATION AND RESPIRABLE MASS CONCENTRATION WITHIN EACH REPETITION UNDER DIFFERENT TEST CONDITIONS

Table C1. The mean of number concentration and respirable mass concentration within each repetition under different test conditions.

Test Condition	Repetition	Number Concentration Mean, particles/cm^3 (SD)	Respirable Mass Concentration Mean, mg/m^3 (SD)
CNTs Percentage (%)			
0	1	436 (41)	0.162 (0.007)
0	2	352 (77)	0.118 (0.005)
0	3	297 (42)	0.117 (0.006)
1	1	288 (74)	0.149 (0.007)
1	2	155 (51)	0.114 (0.031)
1	3	157 (19)	0.123 (0.004)
2	1	310 (30)	0.192 (0.010)
2	2	311 (44)	0.168 (0.008)
2	3	375 (59)	0.158 (0.011)
3	1	418 (73)	0.141 (0.005)
3	2	342 (46)	0.130 (0.004)
3	3	259 (71)	0.104 (0.037)
4	1	431 (114)	0.329 (0.081)
4	2	400 (40)	0.373 (0.014)
4	3	531 (78)	0.343 (0.014)
Disc Speed			
Slow	1	94 (5)	0.101 (0.007)
Slow	2	103 (25)	0.116 (0.007)
Slow	3	80 (6)	0.133 (0.006)
Medium	1	310 (30)	0.192 (0.010)
Medium	2	311 (44)	0.168 (0.008)
Medium	3	375 (59)	0.158 (0.011)
Fast	1	3700 (355)	0.332 (0.016)
Fast	2	2940 (321)	0.288 (0.009)
Fast	3	2787 (557)	0.272 (0.009)
Sandpaper Type			
Coarse	1	4000 (1174)	0.228 (0.008)
Coarse	2	4870 (1225)	0.192 (0.042)
Coarse	3	5140 (966)	0.203 (0.008)
Medium	1	310 (30)	0.192 (0.010)
Medium	2	311 (44)	0.168 (0.008)

Medium	3	375 (59)	0.158 (0.011)
Fine	1	99 (6)	0.532 (0.033)
Fine	2	237 (79)	0.580 (0.033)
Fine	3	307 (133)	0.558 (0.041)
Test Samples			
2% CNTs	1	310 (30)	0.192 (0.010)
2% CNTs	2	311 (44)	0.168 (0.008)
2% CNTs	3	375 (59)	0.158 (0.011)
Sample 1	1	720 (76)	0.198 (0.013)
Sample 1	2	256 (39)	0.185 (0.008)
Sample 1	3	392 (55)	0.169 (0.010)
Sample 2	1	1480 (369)	0.186 (0.014)
Sample 2	2	1140 (256)	0.155 (0.010)
Sample 2	3	1780 (262)	0.168 (0.010)

Table C1 continued.